Regulatory mechanisms of neural stem cell proliferation by hypoxia-inducible factor

Huang Zhenyu

Laboratory of Regulation of Neuronal Development
Institute for Protein Research
Osaka University

Contents

Abstract

Neural stem cells (NSCs) reside in vivo in hypoxic environments, and NSC proliferation is enhanced in vitro under hypoxic conditions. Various adaptive responses to hypoxia are mediated by hypoxia-inducible factors (HIFs), a family of basic helix-loop-helix Per-Arnt-Sim (PAS) transcription factors. Necdin, a MAGE (melanoma antigen) family protein, is expressed abundantly in postmitotic neurons and possesses potent anti-mitotic and anti-apoptotic activities. We here report that hypoxia induces degradation of the necdin protein in primary NSCs by HIF-mediated ubiquitin-proteasome system. Necdin was expressed in primary NSCs prepared from the ganglionic eminences of mouse embryos. Hypoxia enhanced neurosphere formation of NSCs, in which the necdin protein level was significantly reduced. Primary NSCs prepared from necdin-deficient mice exhibited higher rates of proliferation and apoptosis than those from wild-type mice in normoxia, whereas there were no significant differences in the proliferation and apoptosis rates between necdin-deficient and wild-type NSCs in hypoxia. HIF-2α was predominantly expressed in hypoxic NSCs, where expression of HIF-responsive genes was upregulated. HIF-2α interacted with necdin via its PAS domain, which enhanced necdin ubiquitination. Lentivirus-mediated expression of the PAS domain in primary NSCs promoted necdin degradation and enhanced NSC proliferation in normoxia, whereas a small-molecule inhibitor of HIF-2α translation stabilized the necdin protein and reduced NSC proliferation in hypoxia. These results suggest that oxygen tension regulates the necdin protein level in NSCs through HIF-2α-mediated proteasomal degradation to modulate their proliferation and apoptosis.

[Publication]

Zhenyu H, Fujiwara K, Minamide R, Hasegawa K, Yoshikawa K (2013) Necdin controls proliferation and apoptosis of embryonic neural stem cells in an oxygen tension-dependent manner. *J Neurosci* 33(25): 10362-10373

Introduction

The mammalian brain is the most metabolically active organ and requires large amounts of oxygen for its physiological function. Oxygen availability is crucial for the energy metabolism in neurons, where a large amount of ATP is utilized for their function and survival. Although mammalian brain accounts for a very small percentage of our body weight, but it is indispensable for the most crucial activities in our life. There existed a large difference of the oxygen consumption between different organs. Especially, the part pressure and concentration of oxygen in the brain are considerably lower and non-uniform (Erecinska and Silver, 2001). In embryonic brain in vivo, oxygen tensions are particularly low in the ventricular zone, where NSCs reside. Pimonidazole adducts were used to investigate the oxygen tensions in E11.5 embryonic brain. In the ventricular zone, pimonidazole adducts were clearly observed, which suggest that oxygen tensions are particularly low (Mutoh et al., 2012). An accumulating body of evidence suggests that hypoxia enhances the expansion of embryonic NSCs or neuronal progenitors in vitro (Studer et al., 2000; Zhao et al., 2008; Chen et al., 2010). The growth potential of neural crest stem cells were tested at 5% $O_{2,}$ which had been considered very close to physiological oxygen levels. A high population of stem cells was observed under these conditions (Morrison et al., 2000). Rat NSCs in hypoxic conditions is regulated by modulation of cell cycle through increased expression of cyclin D1, which is, in turn, mediated through JNK signaling (Chen et al., 2007). Low oxygen can also inhibit NSCs death and further influence the proliferation (Clarke and van der Kooy, 2009). Notch, whose activation is modulated by HIF-1α in response to hypoxia, was also required to maintain the undifferentiated cell state of NSCs. Increased proliferation of embryonic stem cells-derived NSCs in hypoxic conditions has also been reported (Rodrigues et al., 2010). These observations raise the possibility that hypoxia

is indispensable for the high proliferation activity of NSCs.

Cellular responses to hypoxia are often mediated by hypoxia-inducible factors (HIFs), which regulate oxygen-dependent transcription of various genes involved in oxygen and energy homeostasis (Greer et al., 2012). HIF-1α and HIF-2α are basic helix-loop-helix PAS transcription factors that share a high degree of sequence identity. HIF-1α influences the expansion and cell fate switching of NSCs during development (Zhao et al., 2008; Panchision, 2009; Mazumdar et al., 2010; Mutoh et al., 2012). Among early adaptive responses to hypoxia, HIF-1α and HIF-2α have been characterized as the main regulators of oxygen-dependent gene transcription that modulate oxygen and metabolic supply upon hypoxic exposure. HIF-1α is widely expressed. HIF-2α as a HIF-α subunit is assumed to differ from HIF-1α, it has target gene specificity and tissue-specific function. HIF-α can formed the heterodimer with HIF-β. They undergo proteolytic regulation that is dependent on the presence of independently functioning oxygen-dependent degradation domains (ODD), which are located in the central region of the molecule. HIF also possess two transactivation domains, an internal activation domain (NAD) and a carboxy-terminal activation domain (CAD). HIFs are rapidly degraded through the ubiquitin-proteasome pathway under normoxic conditions. Hypoxia initiates stabilization of the HIF-α subunit and initiate the transcription of specific target genes. Nowadays, the expression levels of HIF-1α and HIF-2α in the brain have already been convinced. Growing stem or neuronal progenitor cells under low oxygen concentration, with HIF-1α activation, appears to improve cell proliferation, neuronal differentiation or both. While HIF-1α has been extensively studied, HIF-2α should be targeted relative to stem cell proliferation and differentiation. Possibly HIF-2α biological activity might explain the differences concerning the control of proliferation versus differentiation by hypoxia.

Therefore, more data are necessary to disclose the role of oxygen in the cellular pathways related to proliferation and to differentiation. The molecular mechanisms whereby HIF proteins are involved in the regulation of NSC proliferation remain elusive at the present time.

Necdin is a pleiotropic protein expressed abundantly in postmitotic neurons (Maruyama et al., 1991; Uetsuki et al., 1996). Necdin interacts with many regulatory proteins and serves as a hub of protein-protein interaction networks (Lavi-Itzkovitz et al., 2012). Ectopic expression of necdin strongly suppresses the proliferation of cell lines. Cell growth was arrested by stably transfected necdin into NIH3T3 cells (Hayashi et al., 1995). By interaction with the tumor suppressor protein p53, necdin can also perform a role as a grow suppressor and modulate the biological functions in postmitotic neurons (Taniura et al., 1998). Necdin, like MAGE G1 (The melanoma antigen G1), can target both E2F1 and p75 to modulate cell viability during the development of brain (Kuwako et al., 2004). The MAGE homology domain (MHD) of necdin had been determined to interact with p53 and required for cell growth suppression (Taniura et al., 2005). Necdin, like retinoblastoma protein, targets cellular E2F transcription factors and affect the cell cycle (Taniura et al., 1998; Kobayashi et al., 2002). Furthermore, necdin suppresses oxidative damage-induced neuronal apoptosis by interacting with p53 (Taniura et al., 1999). By forming a stable complex with p53 and Sirt1, necdin can downregulate p53 acetylation levels, which further protect neuron form DNA damage-induced apoptosis (Hasegawa and Yoshikawa, 2008). Recent studies have shown that necdin and its homologous proteins such as NRAGE (MAGE-D1), magphinin (MAGE-D4) and MAGE-G1 suppress cell growth. Intriguingly, necdin interacts with HIF-1α and negative regulates the stability of HIF-1α and neuronal function (Moon et al., 2005; Friedman and Fan, 2007), suggesting

that the interaction between necdin and HIF-1α affects cell proliferation and apoptosis under hypoxic conditions.

Several lines of evidence indicate that necdin is expressed in multipotent stem cells or committed progenitors of mesodermal/mesenchymal origin such as mesoangioblast stem cells. The transcription factors Msx2 and necdin perform a crucial role in regulating smooth muscle differentiation (Brunelli et al., 2004). For brown adipocyte precursors, a key signaling network involved in necdin has defined for brown preadipocyte determination (Tseng et al., 2005). The function of necdin also be found in skeletal muscle satellite cells, which show the importance of necdin in muscle generation (Deponti et al., 2007). The excessive proliferation of hematopoietic stem cell during hematopoietic regeneration can be prevented by necdin (Kubota et al., 2009). Together with p53, necdin also can control the cell cycle entry of hematopoietic stem cells (Liu et al., 2009). During adipose tissue development, necdin can prevent excessive preadipocyte proliferation and control white adpocyte number (Fujiwara et al., 2012). However, little is known about the expression and function of necdin in mammalian NSCs.

The present study provides evidence that hypoxic conditions can facilitate degradation of necdin and enhance the proliferation of cultured NSCs. Under normoxic conditions (20% O_2), the proliferation is significantly enhanced in necdin-deficient NSCs. Interestingly, hypoxia significantly down regulate the protein levels of necdin, which indicating that necdin is implicated to be involved in the proliferation of NSCs cultured under hypoxic conditions. We also revealed that both mRNA and protein levels of HIF-2α were higher than HIF-1α in NSCs cultured under hypoxic conditions (2% O_2). The close interplay between necdin and HIF-2α was demonstrated, which can facilitate the ubiquitination of necdin, and targeting it for proteasomal degradation. The

present study suggests that HIF-2α down regulate the expression levels of necdin and cause the degradation, which further affect the proliferation of NSCs cultured under hypoxic conditions (figure 18). The present findings provide insights into the molecular mechanism that controls the proliferation rates of NSCs under different oxygen tensions.

Materials and methods

Animals

Necdin gene (*Ndn*) mutant mice (Ndn^{tm1Ky}) were generated and maintained as described previously (Kuwako et al., 2005). Heterozygous male mice ($Ndn^{+/-}$)(>20 generations in ICR background) were crossed with wild-type female mice ($Ndn^{+/+}$) to obtain wild-type ($Ndn^{+m/+p}$) and paternal *Ndn*-deficient ($Ndn^{+m/-p}$) littermates. Genotypes of all mice were analyzed by PCR for mutated *Ndn* locus. Experiments using gene-targeted mice were approved by the Recombinant DNA and Animal Experiment Committees of the Institute for Protein Research, Osaka University, and performed in accordance with institutional guidelines and regulations.

Neural stem cells

Primary NSCs were prepared from striatal primordia (also known as ganglionic eminences, GEs) of mice at embryonic day 14.5 (E14.5) (Reynolds et al., 1992). GEs from wild-type and necdin-deficient ($Ndn^{+m/-p}$) mice were dissected, incubated for 5 min at 37°C in Ca^{2+}/Mg^{2+} -free glucose-supplemented Hanks' balanced salt solution with 0.05% trypsin, dissociated in DMEM supplemented with 10% fetal bovine serum, and centrifuged at 200 x g for 3 min. The cell pellet was resuspended and incubated for 6 d at 37°C under humidified 5% CO_2 conditions in DMEM/F12 medium (GIBCO) supplemented with 14 mM sodium bicarbonate, 1 mM N-acetyl-L-cysteine, 33 mM D(+)-glucose, 1 mg/ml bovine serum albumin (Sigma-Aldrich), 2 mM L-glutamine, 20 ng/ml EGF (PeproTech), 20 ng/ml FGF (PeproTech) and B27 (GIBCO). Floating spheres were collected and used as primary NSCs for the following experiments. For cultures in hypoxic conditions, primary NSCs were incubated at 37°C under 2% O_2/5% CO_2 conditions in a multi-gas incubator (MCO-5M, Panasonic). For differentiation,

primary neurospheres were dissociated with StemPro Accutase (Invitrogen) and plated onto poly-L-ornithine-coated coverslips in growth factor-deprived DMEM/F12 medium for 5 d.

Immunostaining

Frozen 12-μm-thick tissue sections were prepared from ICR mouse embryos at E14.5 and immunostained as described previously (Kuwajima et al., 2004). For immunocytochemistry, primary NSCs, dispersed NSCs and differentiated cells were fixed with 10% formalin solution at room temperature for 20 min and then permeabilized with methanol at room temperature for 20 min. Samples were incubated at 4°C overnight with primary antibodies and fluorescence dye-conjugated secondary antibodies at room temperature for 90 min. Primary antibodies used are : rabbit polyclonal antibodies against necdin (NC243; 1:1000), nestin (ST-1; 1:000)(Aizawa et al., 2011), guinea pig polyclonal antibody against necdin (GN1; 1:1000)(Kuwako et al., 2005) and Dlx2 (GDlx2, 1:3000)(Kuwajima et al., 2006), mouse monoclonal antibodies against Sox2 (1:500; R&D), βIII-tubulin (1:1000; Promega) and GFAP (1:1000) (gift from Dr. Seiichi Haga, Tokyo Metropolitan Institute of Medical Science). Secondary antibodies are: anti-rabbit, anti-guinea pig, and anti-mouse IgGs conjugated with cyanine 3 and cyanine 2 (1:500; Jackson ImmunoResearch). Chromosomal DNA was detected with 3.3 μM Hoechst 33342 (Sigma-Aldrich). The images were observed with a fluorescence microscope (MZ16 F; Leica Microsystems) or a fluorescence microscope (BX-50-34-FLAD1; Olympus Optical), taken by charge-coupled device camera system (DP70; Olympus Optical), and processed using Adobe PhotoShop CS5.

Western blot analysis

Cells were homogenized with a lysis buffer containing 10 mM Tris-HCl (pH 8.0), 150 mM NaCl, 1 mM EDTA, 1% Nonidet P-40, 10% glycerol, and a protease inhibitor cocktail (Complete, Roche). The protein concentration was determined by the Bradford method (Bio-Rad). Proteins (10 μg/lane) were separated by 10% SDS-PAGE, and electroblotted to polyvinylidene difluoride membranes (Immobilon, Millipore). Membranes were blocked with skim milk in phosphate buffered saline/0.05 % Tween-20, and incubated with primary antibodies against necdin (NC243; 1:3000), actin (JLA20; 1:200; DSHB), β-tubulin (1:1000; MP Biomedicals), Sox2 (1:500; R&D system), CD133 (1:500; eBioscience), HIF-1α (1:500; R&D systems), HIF-2α (sc-28706; 1:400; Santa Cruz). Flag (M2; 1:500; Sigma-Aldrich), Myc (9E10; 1:10), PCNA (PC10; 1:500; Santa Cruz), ubiquitin (FK2; 1:1000; Enzo Life Sciences) and Cdc2 (sc-54; 1:300; Santa Cruz). The membrane was incubated with horseradish peroxidase-conjugated IgG (Cappel). Proteins were visualized by Western Lightning Plus-ECL (PerkinElmer, Inc.). Signal intensities were quantified with an image analyzer (LAS-1000 Plus; Fuji Film) and ImageJ 1.44 software. Lysates of hypoxic HEK293A cells treated with 100 μM $CoCl_2$ and 10 μM MG132 (Peptide Institute) for 12 h were used as controls of HIF proteins.

Neurosphere assay

The efficiency of neurosphere formation was determined on the basis of the study described previously (Reynolds and Weiss, 1996). Briefly, primary NSCs were treated with StemPro Accutase, dispersed into single cells, and resuspended in DMEM/F12 medium with the supplements described above. Dispersed cells (150 cells per well) were plated in 96-well plates (Thermo Fisher Scientific) and cultured for 5 d in normoxia or hypoxia. Neurospheres were observed with an inverted microscope

(Olympus IX70), and images were captured. The diameters of individual neurospheres were measured using ImageJ 1.44 software. Neurospheres of >20 μm in diameter were counted and divided into three categories (20-40 μm, 40-60 μm, and > 60 μm in diameter). To inhibit endogenous HIF-2α expression, NSCs cultured for 6 d were treated with HIF-2α Translation Inhibitor (Calbiochem) (Zimmer et al., 2008) under hypoxic conditions for 3 d (for Western blot analysis) or for 5 d (for neurosphere assay).

Purification of NSCs

NSCs were purified using anti-CD133 antibody-coupled microbeads as CD133 (also known as prominin) has often been used to isolate neural stem cells (Uchida et al., 2000; Pfenninger et al., 2007). After dissection, cells were centrifuged at 300 x g for 10 min and washed with PBS containing 0.5% BSA (AlbuMAX; Invitrogen) and 2 mM EDTA. Pellets were suspended with 80 μl wash buffer and mixed with anti-CD133-coupled microbeads (2 μl for $1x10^6$ cells) (Miltenyi Biotec). The mixture were incubated for 15 min at 4°C and separated on a magnetic column (Miltenyi Biotech). Cells bound to the microbeads ($CD133^+$) and unbound cells ($CD133^-$) were resuspended in DMEM/F12 containing 2 mM L-glutamine, B27, 20 ng/ml EGF and 20 ng/ml FGF, incubated for 5 d, and subjected to the neurosphere assay.

Cell proliferation assay

For BrdU incorporation assay, primary NSCs (6 d culture) were incubated in hypoxic conditions for 24 h, labeled with 10 μM BrdU for 4 h, dissociated into single cells, and plated onto the poly-L-ornithine-coated coverslips in 24-well plates (5×10^4 cells per well). BrdU incorporation assay was performed as described previously (Taniura et al., 1999; Fujiwara et al., 2012). Cells were incubated with mouse monoclonal anti-BrdU

antibody (1:30, Roche) and anti-nestin (ST-1; 1:1000) antibody for 1 h at room temperature, and incubated with second antibody against IgGs conjugated with cyanine 2 and cyanine 3, respectively, and counterstained with Hoechst 33324. BrdU-labelled cells among nestin-immunopositive cells were counted by fluorescence microscopy.

For cell proliferation assay in vivo, pregnant mice were injected i.p. with ethynyl deoxyuridine (EdU, Invitrogen)(50 mg/kg body weight) at day 14.5 of gestation, and forebrain tissues were fixed 2 h later. Incorporated EdU was detected using Click-iT EdU Alexa Fluor Imaging Kit (Invitrogen). The fluorescence intensity was quantified by fluorescence microphotometry as described previously (Hasegawa et al., 2012). Briefly, fluorescence images (12-bit digital monochrome images) were captured with a CCD camera (CoolSNAP monochrome; Nippon Roper). EdU fluorescence intensity in the GE ventricular/subventricular zone was analyzed using fluorescence image analysis software (Fluoroimage Cool V; Mitani). The background intensity of the equal-sized adjacent area without EdU signals was subtracted from the intensity of EdU signal-containing area.

Apoptosis assay

Nuclear DNA fragmentation was analyzed by terminal deoxynucleotidyl transferase-mediated biotinylated UTP nick end labeling (TUNEL) visualized with Texas Red (Gavrieli et al., 1992; Uetsuki et al., 1999). Primary NSCs (6 d culture) were dispersed and incubated in normoxic (20% O_2) or hypoxic conditions (2% O_2) for 24 h. NSCs were dispersed, plated onto poly-L-ornithine-coated coverslips in 24-well plates (5 x 10^4 cells per well), fixed 6 h after plating, and subjected to TUNEL analysis. Chromosomal DNA was counterstained with 3.3 μM Hoechst 33342. TUNEL analysis in brain tissues was carried out as described previously (Kuwako et al., 2005). TUNEL-positive cells in the proliferative zone of dorsal GE were counted and

quantified as the number in the equal-sized area.

Quantitative RT-PCR

Total RNA was extracted from NSCs with phenol and guanidine thiocyanate mixture (TRI Reagent, Molecular Research Center), and genomic DNA was digested with RQ1 RNase-free DNase (Promega). cDNA was synthesized from total RNA (2 μg) using Transcriptor First Strand cDNA Synthesis Kit (Roche). cDNA (10 ng) was used as templates for PCR. Primers used for real-time PCR are as follows: *HIF-1α* (forward, 5'-ggacaagtcaccacagga-3'; reverse, 5'-ggagaaaatcaagtcgtg-3'); *HIF-2α* (forward, 5'-ccaaggggcaggtggtat-3'; reverse, 5'-cacgtcgttcttctcgatctca-3'); *Vegf* (forward, 5'-ccccgacgagatagagta-3'; reverse, 5'-gctttggtgaggtttgat-3'); *Glut1* (forward, 5'-tcaacacggccttcactg-3'; reverse, 5'- cacgatgctcagataggacatc-3'); *Cyclin D1* (forward, 5'-ccaacaacttcctctcctgc -3'; reverse, 5'- agaccagcctcttcctccac-3'); *erythropoietin* (forward, 5'-catctgcgacagtcgagttctg-3'; reverse, 5'-cacaacccatcgtgacattttc-3'); *Cdc2* (forward, 5'- caaaatagagaaaattggagaaggtac-3'; reverse, 5'-agattttgaggttttaagtctctgtga-3'). RT-PCR products were quantified using a real-time PCR instrument (LightCycler, Roche) and FastStart DNA MasterPLUS SYBR Green I kit (Roche). Melting curves were analyzed to confirm a single species of each PCR product. *α-Actin* cDNA was used as an internal standard to quantify the relative expression of each cDNA. Values of *HIF-1α* and *HIF-2α* were corrected with PCR efficiencies using equal amounts of full-length *HIF-1α* and *HIF-2α* cDNAs.

Co-immunoprecipitation

HEK293A cells were transfected with expression vectors and harvested 24 h later. Cell lysates were subjected to co-immunoprecipitation assay as described previously (Hasegawa et al., 2012). cDNA encoding mouse full-length HIF-2α was cloned from

NSCs cultured under hypoxic conditions. For Myc-tagged protein expression, full-length HIF-2α, the PAS domain (HIF-2α 97-341), TAD (transactivation domain)(HIF-2α 490-874) and ODD (oxygen-dependent degradation) domain (HIF-2α 516-686) were subcloned into 6xMyc-pcDNA3.1. cDNA encoding the N-terminal domain (necdin 1-100) and the MAGE homology domain (necdin 101-300) of necdin were subcloned into p3xFLAG-CMV14 (Sigma-Aldrich). Expression vectors for necdin and Myc-tagged p53 were described previously (Taniura et al., 1999). The cells were harvested 24 h after transfection and lysed in the lysis buffer. Proteins in the lysates (150 μg) were incubated at 4°C for 2 h with antibodies against Flag (M2; 1:50; Sigma), Myc (9E10; 1:4) and necdin (NC243; 1:100), pelleted with protein A-Sepharose (GE Healthcare), and detected by Western blotting. For detection of endogenous complex of necdin and HIF-2α, nuclear lysates (1 mg) of E14.5 mouse forebrain were incubated with guinea pig anti-necdin antibody (GN1)(1:100)(Kuwako et al., 2005), pelleted with Dynabeads Protein A (Invitrogen), separated by 7.5% SDS-PAGE, and detected by Western blotting with antibodies against HIF-2α, PCNA (PC10; Santa Cruz; 1:500) and necdin (NC243; 1:3000).

In vitro binding assay

pMALC2 plasmids carrying cDNAs for HIF-2α and its deletion mutants were constructed for the MBP fusion proteins. In vitro binding assay was performed as described previously (Hasegawa and Yoshikawa, 2008). Briefly, MBP-HIF-2α fusion proteins were affinity purified with amylose resin (New England Biolabs). Purified MBP-HIF-2α fusion protein (2 μg) bound to amylose resin was incubated with purified His-tagged necdin (200 ng) at 4°C for 30 min in 0.5 ml of binding buffer (20 mM Tris-HCl (pH 7.5), 200 mM NaCl, and 1 mM EDTA). The resin was washed with the binding buffer, and bound proteins were eluted with 20 mM maltose. His-tagged necdin

was detected by Western blotting.

Ubiquitination assay

HEK293A cells were transfected with expression vectors for Myc-tagged proteins, necdin and Flag-ubiquitin by the calcium phosphate method and harvested 24 h later following treatment with 10 μM MG132 for 3 h before harvest. Flag-ubiquitin-conjugated necdin was immunoprecipitated with anti-necdin antibody (NC243; 1:100) and detected by immunoblotting with anti-Flag monoclonal antibody (M2; 1:500; Sigma). For detecting endogenous necdin ubiquitination, NSCs were infected with lentivirus vectors, incubated for 6 d, and harvested. Ubiquitin-conjugated necdin was immunoprecipitated with anti-necdin antibody (NC243; 1:100), separated by 10% SDS-PAGE, and detected by Western blotting with anti-ubiquitin antibody (FK2).

Recombinant lentiviruses

Recombinant lentiviruses were produced by HEK293FT cells transfected with viral DNA and two helper plasmids as described previously (Miyoshi et al., 1998; Fujiwara et al., 2012). cDNAs for Flag-tagged HIF-2α PAS and ODD domains were subcloned into pENTR1A entry vector (Invitrogen) to construct the destination vector CSII-CMV-RfA-PAS-IRES2-DsRed-Express2, in which DsRed-Express2 (Clontech) was inserted as an expression indicator. For viral infection, lentiviral particles (30 MOI) were added to the dissociated GE cell suspension or isolated $CD133^+$ NSCs, which were subsequently incubated for 6 d.

Statistical analysis

Statistical significance was tested using an unpaired Student's *t* test or one-way

ANOVA followed by Tukey's *post hoc* test. A significance of $p < 0.05$ was required for rejection of the null hypothesis.

Results

Necdin is expressed in primary NSCs

We first examined the expression patterns of necdin and Dlx2, a homeodomain protein required for GABAergic interneuron differentiation, in the GEs of E14.5 mouse by immunohistochemistry (Fig. 1). Necdin was strongly expressed in the septum and cortical marginal zone, whereas the necdin immunoreactivity was very weak in the GE and neocortical ventricular zone, where most of NSCs are located. Double-immunostaining analysis revealed that the GEs contained strongly Dlx2-immunoreactive cells. These expression patterns of necdin and Dlx2 in mouse forebrain are consistent with the previous observations (Kuwajima et al., 2006).

We then examined the expression pattern of necdin in NSCs prepared from the GEs in E14.5 mouse forebrain. Primary NSCs, which were prepared by culturing the GE cells in the presence of growth factors for 6 d, were immunopositive for both necdin and nestin, a neural stem cell marker, and most of the necdin-immunopositive cells overlapped with nestin-immunopositive cells (Fig. 2A). NSCs expressing both Dlx2 and nestin were also observed (Fig. 2B). To characterize the necdin-expressing NSCs, primary neurospheres were dispersed and double-stained for necdin and nestin, Sox2 (another NSC marker), or Dlx2 (Fig. 3A). Necdin was expressed in almost all primary NSCs, whereas the numbers of cells immunopositive for nestin, Sox2, and Dlx2 were smaller than that of necdin-immunopositive cells (necdin, 97 ± 1%; nestin, 86 ± 2%; Sox2, 91 ± 2%; Dlx2, 67 ± 1%: 150 cells analyzed; mean ± SEM; n=3). In most of the NSCs, the necdin immunoreactivity in the cytoplasm was stronger than that in the nucleus. The population of necdin$^+$/Sox2$^+$ cells was the largest among those of double-positive populations (necdin$^+$/Sox2$^+$, 94 ± 3%; necdin$^+$/nestin$^+$, 88 ± 2%; necdin$^+$/Dlx2$^+$, 68 ± 1%: 150 cells analyzed; n=3). Upon withdrawal of the growth

factors from the culture medium, most of the GE-derived NSCs differentiated into neurons and astrocytes as judged by the expression of βIII-tubulin and GFAP, respectively (Fig. 3B), indicating that these NSCs are multipotent. These results suggest that necdin is expressed in embryonic NSCs capable of differentiating into neuronal and glial lineages.

Necdin-deficiency and hypoxia enhance neurosphere formation

We then examined whether the necdin protein level was changed in NSCs cultured in hypoxic conditions. Western blot analysis revealed that a ~42 kDa necdin protein was detected in the NSCs (Fig. 4A). Primary NSCs, which were cultured for 6 d at atmospheric 20% O_2, were incubated for another 3 d at 2% (hypoxia) and 20% O_2 (normoxia). The necdin protein level in hypoxic NSCs was significantly reduced to 42% of those in normoxic NSCs (Fig. 4B, C). On the other hand, the necdin protein was undetected in NSCs prepared from paternal *Ndn*-mutant mice. We then compared the expansion rates of wild-type NSCs cultured under different O_2 conditions by neurosphere assay. The total neurosphere number of necdin-deficient NSCs was significantly larger than that of wild-type NSCs in normoxia, whereas no significant difference in the total cell number was noted between wild-type and necdin-null NSCs in hypoxia (Fig. 5A, B), suggesting that endogenous necdin suppresses NSC proliferation only in normoxia. Analysis of neurosphere size distribution revealed that necdin-deficient NSCs had 4 times the frequency of large-sized neurospheres (>60 μm in diameter) of wild-type NSCs. In contrast, there was no significant difference in each size group was noted between necdin-null and wild-type NSCs in hypoxia (Fig. 5C).

To ascertain whether endogenous necdin modulates proliferation of NSCs, we purified NSCs using anti-CD133 antibody-coupled microbeads, cultured for 6 d, and

subjected to the neurosphere assay. $CD133^+$ NSCs showed a much higher neurosphere formation efficiency than $CD133^-$ NSCs ($CD133^-$ NSCs; 3 ± 0; $CD133^+$ NSCs, 17 ± 2: $p<0.01$), in agreement with the previous findings that CNS-derived $CD133^+$ cells show characteristics of neural stem cells (Uchida et al., 2000; Pfenninger et al., 2007). Necdin and Sox2 were strongly expressed in both $CD133^+$ NSCs and $CD133^-$ NSCs (Fig. 6A). Analysis of neurosphere size distribution revealed a significant increase in neurosphere formation was seen only in large-sized neurospheres (>60 μm in diameter) of necdin-deficient $CD133^+$ NSCs under normoxic conditions (Fig. 6B). These results suggest that hypoxia-induced reduction of endogenous necdin protein level facilitates the proliferation of NSCs.

Necdin-deficient NSCs show high proliferation and apoptosis rates

Necdin-deficient NSCs had more BrdU-positive cells when cultured under normoxic conditions, whereas there was no significant difference between wild-type and necdin-deficient NSCs cultured under hypoxic conditions (Fig. 7A). This indicates that both hypoxia and necdin deficiency enhance the proliferation rates of NSCs. On the other hand, the number of TUNEL-positive apoptotic cells was also increased in necdin-deficient NSCs in normoxia (Fig. 7B). Hypoxia markedly decreased the numbers of apoptotic cells in both wild-type and necdin-deficient NSCs. There was no significant difference in apoptotic cell population between wild-type and necdin-deficient NSCs in hypoxia. These results suggest that hypoxia-induced reduction of endogenous necdin protein level facilitates the proliferation of NSCs.

To examine whether proliferation and apoptosis rates are also increased in the GE in vivo, we carried out the proliferation assay using EdU, a thymidine analog incorporated into nuclear DNA of proliferative cells. The EdU incorporation was increased in the proliferative zones of the GE and cerebral cortex at E14.5 (Data not

shown). Quantification using fluorescence microphotometry revealed a significant increase of EdU incorporation in the GE proliferative zone of necdin-deficient mice (relative fluorescence density: wild-type, 1.0 ± 0.0; necdin-deficient, 1.3 ± 0.1; p <0.025, n=3). The number of TUNEL-positive cells in the GE was also significantly increased in necdin-deficient mice (wild-type, 27 ± 1, necdin-deficient, 41 ± 2; p < 0.005; n=3)(Data not shown). These results suggest that necdin has both anti-mitotic and anti-apoptotic effects on GE cells in vivo.

Primary NSCs predominantly express HIF-2α

To examine whether HIFs were expressed in these primary NSCs, expression levels of *HIF-1α* and *HIF-2α* in normoxic and hypoxic NSCs were analyzed by quantitative RT-PCR (Fig. 8A). In normoxic NSCs, the level of *HIF-2α* mRNA was 9.1 times that of *HIF-1α* mRNA after correction of PCR efficiencies. The *HIF-1α* mRNA level in hypoxic NSCs was significantly increased to 2.5 times that in normoxic NSCs. Western blot analysis of HIF-1α and HIF-2α revealed that only the HIF-2α protein was detected in primary NSCs (6 d culture) incubated for 3 d in hypoxia, in which the necdin level was decreased in wild-type NSCs (Fig. 8B).

We then analyzed the expression levels of HIF-regulated genes in primary NSCs (6 d culture) that were incubated for another 3 d in normoxia or hypoxia. Expression of the HIF-regulated genes *vascular endothelial growth factor* (*Vegf*), *glucose transporter 1* (*Glut1*), and *Cyclin D1* was significantly increased in hypoxic NSCs (5.3, 24.3 and 2.2 times those in normoxic NSCs, respectively)(Fig. 9). Expression of *erythropoietin,* another HIF-regulated gene, was very weak as compared with the expression levels of above genes but was significantly increased in hypoxia (values relative to actin mRNA level; 0.0057 ± 0.0006 in normoxia, 0.0101 ± 0.0005 in hypoxia, p < 0.05). Expression of *Cdc2*, a gene downregulated by necdin (Kurita et al., 2006), in hypoxic

NSCs was 3.2 times the normoxic level. These data suggest that the HIF-2α protein is stabilized and activates its downstream genes in hypoxic NSCs.

Necdin interacts with HIF-2α via the PAS domain

To examine the association between necdin and HIF-2α, we carried out the co-immunoprecipitation assay using transfected HEK293A cells. We first examined the interactions between HIF-2α and necdin using p53 as a positive control. Necdin was co-precipitated with HIF-2α, which was conversely coprecipitated with necdin (Fig. 10A). HIF-2α bound to necdin via the MAGE homology domain (amino acids 101-300), whereas the N-terminal domain (amino acids 1-100), whose sequence is unique to necdin, failed to bind to HIF-2α (Fig. 10B).

To locate the necdin-interacting domain of HIF-2α, deletion mutants including the Myc-tagged PAS domain, oxygen-dependent degradation domain (ODD), transactivation domain (TAD), and full-length HIF-2α were coexpressed with necdin in HEK293A cells for co-immunoprecipitation assay (Fig. 11A). The HIF-2α PAS domain and full-length HIF-2α were co-immunoprecipitated with necdin, whereas neither ODD nor TAD bound to necdin. We then examined the direct interaction between necdin and HIF-2α PAS using MBP-fused HIF-2α domains (expressed in bacteria) and His-tagged necdin (expressed in insect cells)(Fig. 11B). Necdin bound substantially to HIF-2α PAS domain and weakly to the HIF-2α ODD domain. We failed to prepare an intact TAD fragment in the bacterial expression system. These data indicate that necdin interacts directly with HIF-2α PAS domain.

To examine whether an endogenous complex containing necdin and HIF-2α is present under physiological conditions, co-immunoprecipitation assay was carried out using nuclear extracts of E14.5 mouse forebrain. HIF-2α was co-immunoprecipitated with necdin, whereas PCNA, a negative control, failed to be co-precipitated with

necdin. These data suggest that endogenous necdin forms a stable complex with HIF-2α in the mouse forebrain (Fig. 11C).

HIF-2α promotes necdin degradation via the proteasome pathway

To examine whether HIF-2α promotes necdin degradation, we transfected necdin and HIF-2α cDNAs into HEK293A cells and analyzed the necdin protein levels (Fig. 12A). HIF-2α reduced the necdin protein level in a dose-dependent manner (Fig. 12A, lanes 2-4). We also examined whether HIF-2α-dependent decrease in the necdin protein occurs by the proteasome degradation pathway using the proteasome inhibitor MG132 (Fig. 6B). HIF-2α markedly decreased the necdin level (Fig. 12B, lane 4), whereas MG132 increased the levels of both necdin and HIF-2α (Fig. 12B, lane 2). These data suggest that HIF-2α targets necdin for proteasomal degradation. Interestingly, HIF-1α, which have the similar structure to HIF-2α, stabilized necdin protein levels in transfected HEK293A cells (data not shown) .

We then analyzed endogenous levels of necdin and HIF-2α in hypoxic NSCs (Fig. 13A). When primary NSCs were incubated in hypoxia for 24, 48 and 72 h, the necdin protein level was markedly reduced at 72 h, when HIF-2α was clearly detectable (Fig. 13A, lane 4). The necdin protein level in hypoxic NSCs was increased when cultured in the presence of MG132 (Fig. 13B, lanes 3, 4). The necdin level in normoxic NSCs was also increased by MG132 (Fig. 13B, lanes 1, 2). These data suggest that necdin is targeted for proteasomal degradation in primary NSCs, and that necdin undergoes proteasomal degradation even in normoxia.

The HIF-2α PAS domain promotes necdin ubiquitination

We next examined whether HIF-2α promotes necdin ubiquitination, a critical step for proteasomal degradation. Expression vectors for Flag-ubiquitin, Myc-HIF-2α, and

necdin were cotransfected into HEK293A cells, and ubiquitinated necdin was immunoprecipitated with anti-necdin antibody. Although necdin was slightly ubiquitinated in the absence of HIF-2α, its ubiquitination was markedly enhanced by HIF-2α (Fig. 14A). For HIF-1α, we observed totally different phenomenon that necdin ubiquitination was slightly reduced (Data not shown). To examine whether the necdin-interacting PAS domain per se is capable of inducing necdin ubiquitination, the PAS domain and other HIF-2α domains were cotransfected with necdin into the HEK293A cells (Fig. 14B). Only the PAS domain markedly enhanced necdin ubiquitination, and the effect of the PAS domain was stronger than that of full-length HIF-2α.

To examine whether the PAS domain promotes necdin ubiquitination in primary NSCs, we ectopically expressed the PAS domain in NSCs using lentivirus vectors (Fig. 14C). Polyubiquitinated necdin bands were detected even in PAS (-) control, suggesting that endogenous necdin is ubiquitinated in normoxic NSCs. When the PAS-expressing lentivirus was infected into primary NSCs, polyubiquitinated necdin bands at larger molecular sizes (>100 kDa) were enhanced.

The PAS domain promotes both necdin degradation and NSC proliferation

Because the PAS domain is resistant to oxygen-dependent degradation in normoxic conditions, we examined whether lentivirus-mediated expression of the PAS domain in normoxic NSCs induces changes similar to those seen in hypoxic NSCs (Fig. 15A). More than 90% NSC spheres were infected with lentivirus vectors. The necdin protein level in PAS-expressing NSCs was significantly decreased to 58% and 54% of those in empty (DsRed) and ODD-expressing NSCs, respectively, in normoxic conditions, whereas the Cdc2 level in PAS-expressing NSCs was 1.6 and 1.4 times those in NSCs expressing DsRed and ODD, respectively (Fig. 15B, C). We then examined whether

the PAS domain per se modulates neurosphere formation of $CD133^+$ NSCs in normoxic conditions (Fig. 16A). The total neurosphere number of PAS-expressing NSCs was increased to 1.5 and 1.4 times those of NSCs expressing DsRed only and ODD, respectively (Fig. 16A). The numbers of small-sized (20-40 μm in diameter) and large-sized (>60 μm in diameter) neurospheres in the PAS-expressing NSCs were significantly larger than those in ODD-expressing NSCs (Fig. 16B). These data suggest that ectopic expression of the PAS domain mimics the HIF-2α-induced changes seen in hypoxic NSCs such as ubiquitin-mediated degradation of necdin and enhanced NSC proliferation even in normoxic conditions.

To examine the effects of HIF-2α downregulation on the necdin protein level and proliferation rate of NSCs, NSCs were treated with a small-molecule HIF-2α translation inhibitor, which selectively reduces HIF-2α translation by enhancing the binding of Iron-Regulatory Protein 1 to the 5'-untranslated region of HIF-2α mRNA (Zimmer et al., 2008). This inhibitor, which reduced the HIF-2α level and stabilized the necdin protein in hypoxic NSCs (Fig. 17A), significantly reduced the number of large-sized neurospheres (>60 μm in diameter) under hypoxic conditions (Fig. 17B). We also observed the reduced levels of necdin when the protein level of HIF was stabilized by 500 μM and 1 mM DMOG in NSCs cultured under normoxic conditions (Data not shown). This suggests that downregulation of endogenous HIF-2α protein levels stabilizes the necdin protein and downregulates the proliferation rate of NSCs under hypoxic conditions.

Discussion

A considerable amount of the necdin protein was detected in NSCs when cultured in normoxia. Under these conditions, wild-type NSCs exhibited a lower expansion rate than necdin-deficient NSCs, suggesting that endogenous necdin suppresses NSC proliferation. Under hypoxic conditions, the expansion rate of necdin-deficient NSC did not differ significantly from that of wild-type NSCs, in which the necdin protein level was markedly reduced. These findings implicate that hypoxia accelerates NSC proliferation, at least in part, through degradation of endogenous necdin. Because NSCs in developing brain reside in hypoxic environments (Mutoh et al., 2012), the necdin level in NSCs may be kept low in vivo. This suggests little or no difference in the proliferation rate between necdin-deficient NSCs and wild-type NSCs in vivo under physiological conditions. However, we found that EdU incorporation was significantly increased in the GE proliferative zone in vivo of necdin-deficient mice. These results suggest that degradation of the necdin protein in NSCs in vivo through the oxygen tension-dependent system is incomplete as compared with necdin-null conditions. We assume that other complementary mechanisms that modulate the function of necdin are operative in NSCs.

Expansion of NSCs is attributed to increased proliferation, reduced apoptosis, or both. The present study has shown that the hypoxia-promoted expansion of wild-type NSCs is attributed to both increased proliferation and reduced apoptosis as judged by BrdU incorporation assay and TUNEL method, respectively (Fig. 7). Because hypoxia induces a marked reduction of apoptosis, it is suggested that reduced apoptosis of hypoxic NSCs makes a major contribution to their expansion. On the other hand, increased proliferation of necdin-deficient NSCs in normoxia is attributed to increased proliferation, but not to reduced apoptosis. On the contrary, necdin-deficient NSCs in

normoxia showed a significant increase in apoptosis, indicating that necdin has also an anti-apoptotic effect on GE NSCs. Thus, necdin has a dual function that suppresses proliferation and apoptosis of NSCs. In necdin-deficient NSCs, the increased rate of proliferation in normoxia can exceed the increased rate of concurrent apoptosis, resulting in the expansion of NSCs as represented by the increased number of large-sized (>60 μm in diameter) neurospheres. If necdin had no anti-apoptotic effect, expansion of necdin-deficient NSCs would be further augmented in normoxia. These findings suggest that necdin has a strong anti-mitotic activity in embryonic NSCs.

We found necdin-deficient mice show higher rates of proliferation and apoptosis in the GE in vivo than wild-type mice (Data not shown). We have previously reported that GE-derived GABAergic neurons exhibit abnormal differentiation in vivo in necdin-deficient mice at E14.5 (Kuwajima et al., 2006). Tangential migration of Dlx2-positive interneurons is also impaired in the forebrain of necdin-deficient mice at E14.5, and the number of cortical GABAergic interneurons is reduced at postnatal stages (Kuwajima et al., 2010). These mutant mice are highly susceptible to pentylenetetrazole-induced seizures. These findings suggest that hyperproliferation and increased apoptosis of NSCs at early stages of neurogenesis in the GE may lead to the abnormalities of GABAergic interneurons at later stages. Thus, endogenous necdin in GE NSCs may play an important role in normal development of GABAergic interneurons by suppressing both premature mitosis and apoptosis at early stages of neurogenesis.

Although over 25 MAGE family genes have been identified in placental mammals such as mouse and human (Barker and Salehi, 2002), non-mammalian species have only one MAGE gene (Lopez-Sanchez et al., 2007). We have previously reported that Drosophila MAGE, a necdin-homologous MAGE protein, is expressed in neural stem

cells (neuroblasts) and their progeny (ganglion mother cells and postmitotic neurons) during postembryonic neurogenesis (Nishimura et al., 2007). When Drosophila MAGE expression in developing mushroom bodies is downregulated by RNAi-mediated silencing, the population of ganglion mother cells in larval mushroom bodies is significantly increased (Nishimura et al., 2008). In these MAGE-knockdown flies, apoptosis in the neuronal progeny is enhanced during neuronal development. The present findings, together with the previous observations in Drosophila, indicate that necdin and its homologous MAGE are indispensable for the suppression of both proliferation and apoptosis of neuronal precursors. It has also been reported that the single MAGE genes in zebrafish (*Danio rerio*) and chicken (*Gallus gallus*) are expressed predominantly in the CNS proliferative zone and proliferating progenitors of projecting retinal neurons, respectively (Bischof et al., 2003; Lopez-Sanchez et al., 2007). These observations raise the possibility that non-mammalian MAGE proteins also control both proliferation and apoptosis of NSCs and neuronal progenitors.

HIF-1α is expressed in a ubiquitous manner, whereas HIF-2α expression is restricted to specific cell types such as vascular endothelial cells, neural crest cell derivatives, cardiomyocytes, and astrocytes (Wiesener et al., 2003). We found that HIF-2α mRNA is predominantly expressed in primary NSCs. The HIF-2α protein level was reduced in normoxia through oxygen-dependent proteolysis but was stabilized in hypoxia. Although HIF-2α shares a significant sequence homology with well-characterized HIF-1α, there is limited information on the expression and function of HIF-2α in NSCs. In zebrafish, HIF-2α is predominantly expressed in neural stem cell population of the neural tube during development, and morpholino-mediated knockdown of HIF-2α causes abnormal CNS development (Ko et al., 2011). Because necdin-homologous MAGE is expressed in developing zebrafish CNS (Bischof et al.,

2003), the present findings may help understand the molecular mechanisms underlying the control of proliferation and differentiation of vertebrate NSCs through the interplay between HIF-2α and necdin or non-mammalian MAGE.

In hypoxic NSCs, expression levels of the HIF-regulated genes *Vegf*, *Glut1*, *Cyclin D1,* and *erythropoietin* were significantly increased, indicating that HIF-induced transcription is activated in hypoxia. It has previously been reported that expression of *Vegf*, *erythropoietin*, and *Cyclin D1* is upregulated in NSCs under hypoxic conditions (Studer et al., 2000; Chen et al., 2010). The enhanced proliferation of NSCs is also supported by the increased expression of *Cdc2* and *Cyclin D1*, both of which promote the cell cycle. It is noteworthy that *Cdc2* expression is strictly downregulated by necdin in cerebellar granule neurons (Kurita et al., 2006). It has previously been shown that hypoxia-induced reduction of apoptosis contributes primarily to the enhanced expansion of hypoxic NSCs (Clarke and van der Kooy, 2009). Because Vegf significantly promotes the survival of embryonic neural stem cells (Wada et al., 2006), it is possible that the increased *Vegf* expression in hypoxic NSCs leads to the reduction of apoptosis.

Although there is a large amount of information about the molecular mechanisms underlying ubiquitin-dependent degradation of HIFs (Greer et al., 2012), little is known about the involvement of HIFs in the ubiquitin-dependent degradation of their target proteins. It has recently been reported that HIF-1α negatively controls regulatory T cell development by binding Foxp3 and targeting it for proteasomal degradation (Dang et al., 2011). Similarly, as shown presently, HIF-2α enhances the ubiquitination of necdin and induces its proteasomal degradation. Notably, necdin interacts preferentially with the PAS domain of HIF-2α. The PAS domains are present in many proteins and serve as important signaling modules that mediate the protein-protein

interactions in response to various external and internal stimuli (Taylor and Zhulin, 1999). We are currently investigating whether the HIF-2α PAS domain serves as a platform that promotes necdin ubiquitination by recruiting a protein or a multiprotein complex possessing E3 ubiquitin ligase activity.

It has been previously reported that HIF-1α negatively regulates regulatory T cell development by binding Foxp3 and targeting it for proteasomal degradation. In the present study, we found very similar phenomenon that HIF-2α can regulate the proliferation of NSC by binding to necdin and targeting it for proteasomal degradation. The consistency of the results implicates that HIF protein may recruit E3-ligase complex and affects the ubiquitination and degradation of some protein like Foxp3 and necdin. RING-type E3 enzymes are bridging factors that bring the E2 enzyme with its activated ubiquitin into the vicinity of the substrate, some necdin binding RING-type E3-ligases such as Parkin, Nse1, Mdm2 and Ube3a were cloned and applied to investigate the specific E3 ligase of necdin (data not shown). Unfortunately, none of them can facilitate the ubiquitination of necdin individually. PAS domain of HIF-2α can significantly elevate the ubiquitination of necdin. Thus, we propose that the E3-ligase complex of necdin can be recruited by PAS domain of HIF-2α. Here, the PAS domain can be a mimic of HIF-2α that facilitate the ubiquitination of necdin and target it for proteasome-dependent degradation or even accelerate the proliferation of NSCs.

Necdin is expressed in stem cells or progenitors residing in non-neuronal tissues (Brunelli et al., 2004; Tseng et al., 2005; Deponti et al., 2007; Kubota et al., 2009; Liu et al., 2009; Fujiwara et al., 2012). Necdin is located in the nucleus of adipose tissue-derived mesenchymal stem cells in an undifferentiated state, and adipogenic stimuli downregulate the nuclear necdin level prior to the proliferation of committed adipocyte progenitors (Fujiwara et al., 2012), suggesting that nuclear necdin is degraded

by proteolysis in response to adipogenic stimuli. Cell cycle-related proteins are often degraded in a stage-dependent manner by the ubiquitin-proteasome system. Similarly, the nuclear necdin level in NSCs is controlled in an oxygen tension-dependent manner by the ubiquitin-proteasome system. We have also found that necdin is expressed in NSCs residing in the ventricular/subventricular zone of the neocortex during embryonic development, and that both proliferation and apoptosis of these NSCs are increased in vivo in necdin-null mice (R. Minamide and K. Yoshikawa, unpublished observations). We assume that nuclear necdin level is strictly regulated in NSCs that occupy microenvironments containing different oxygen levels in the embryonic brain. Further studies on the posttranslational modifications of the necdin protein will provide valuable insight into the physiological controls of the proliferation of NSCs during neurogenesis.

References

Aizawa T, Hasegawa K, Ohkumo T, Haga S, Ikeda K, Yoshikawa K (2011) Neural stem cell-like gene expression in a mouse ependymoma cell line transformed by human BK polyomavirus. Cancer Sci 102:122-129.

Barker PA, Salehi A (2002) The MAGE proteins: Emerging roles in cell cycle progression, apoptosis, and neurogenetic disease. J Neurosci Res 67:705-712.

Bischof JM, Ekker M, Wevrick R (2003) A MAGE/NDN-like gene in zebrafish. Dev Dyn 228:475-479.

Brunelli S, Tagliafico E, De Angelis FG, Tonlorenzi R, Baesso S, Ferrari S, Niinobe M, Yoshikawa K, Schwartz RJ, Bozzoni I, Cossu G (2004) Msx2 and necdin combined activities are required for smooth muscle differentiation in mesoangioblast stem cells. Circ Res 94:1571-1578.

Chen HL, Pistollato F, Hoeppner DJ, Ni HT, McKay RD, Panchision DM (2007) Oxygen tension regulates survival and fate of mouse central nervous system precursors at multiple levels. Stem Cells 25:2291-2301.

Chen X, Tian Y, Yao L, Zhang J, Liu Y (2010) Hypoxia stimulates proliferation of rat neural stem cells with influence on the expression of cyclin D1 and c-Jun N-terminal protein kinase signaling pathway in vitro. Neuroscience 165:705-714.

Clarke L, van der Kooy D (2009) Low oxygen enhances primitive and definitive neural stem cell colony formation by inhibiting distinct cell death pathways. Stem Cells 27:1879-1886.

Dang EV, Barbi J, Yang HY, Jinasena D, Yu H, Zheng Y, Bordman Z, Fu J, Kim Y, Yen HR, Luo W, Zeller K, Shimoda L, Topalian SL, Semenza GL, Dang CV, Pardoll DM, Pan F (2011) Control of T(H)17/T(reg) balance by

hypoxia-inducible factor 1. Cell 146:772-784.

Deponti D, Francois S, Baesso S, Sciorati C, Innocenzi A, Broccoli V, Muscatelli F, Meneveri R, Clementi E, Cossu G, Brunelli S (2007) Necdin mediates skeletal muscle regeneration by promoting myoblast survival and differentiation. J Cell Biol 179:305-319.

Erecinska M, Silver IA (2001) Tissue oxygen tension and brain sensitivity to hypoxia. Respir Physiol 128:263-276.

Friedman ER, Fan CM (2007) Separate necdin domains bind ARNT2 and HIF1alpha and repress transcription. Biochem Biophys Res Commun 363:113-118.

Fujiwara K, Hasegawa K, Ohkumo T, Miyoshi H, Tseng YH, Yoshikawa K (2012) Necdin controls proliferation of white adipocyte progenitor cells. PLoS ONE 7:e30948.

Gavrieli Y, Sherman Y, Ben-Sasson SA (1992) Identification of programmed cell death in situ via specific labeling of nuclear DNA fragmentation. J Cell Biol 119:493-501.

Greer SN, Metcalf JL, Wang Y, Ohh M (2012) The updated biology of hypoxia-inducible factor. EMBO J. 31: 2448-2460Hasegawa K, Yoshikawa K (2008) Necdin regulates p53 acetylation via Sirtuin1 to modulate DNA damage response in cortical neurons. J Neurosci 28:8772-8784.

Hasegawa K, Yoshikawa K (2008) Necdin regulates p53 acetylation via Sirtuin1 to modulate DNA damage response in cortical neurons. J Neurosci 28: 8772-8784.

Hasegawa K, Kawahara T, Fujiwara K, Shimpuku M, Sasaki T, Kitamura T, Yoshikawa K (2012) Necdin controls foxo1 acetylation in hypothalamic arcuate neurons to modulate the thyroid axis. J Neurosci 32:5562-5572.

Hayashi Y, Matsuyama K, Takagi K, Sugiura H, Yoshikawa K (1995) Arrest of cell

growth by necdin, a nuclear protein expressed in postmitotic neurons. Biochem Biophys Res Commun 213:317-324.

Ko CY, Tsai MY, Tseng WF, Cheng CH, Huang CR, Wu JS, Chung HY, Hsieh CS, Sun CK, Hwang SP, Yuh CH, Huang CJ, Pai TW, Tzou WS, Hu CH (2011) Integration of CNS survival and differentiation by HIF2alpha. Cell Death Differ 18:1757-1770.

Kobayashi M, Taniura H, Yoshikawa K (2002) Ectopic expression of necdin induces differentiation of mouse neuroblastoma cells. J Biol Chem 277:42128-42135.

Kubota Y, Osawa M, Jakt LM, Yoshikawa K, Nishikawa S (2009) Necdin restricts proliferation of hematopoietic stem cells during hematopoietic regeneration. Blood 114:4383-4392.

Kurita M, Kuwajima T, Nishimura I, Yoshikawa K (2006) Necdin downregulates cdc2 expression to attenuate neuronal apoptosis. J Neurosci 26:12003-12013.

Kuwajima T, Nishimura I, Yoshikawa K (2006) Necdin promotes GABAergic neuron differentiation in cooperation with Dlx homeodomain proteins. J Neurosci 26:5383-5392.

Kuwajima T, Hasegawa K, Yoshikawa K (2010) Necdin promotes tangential migration of neocortical interneurons from basal forebrain. J Neurosci 30:3709-3714.

Kuwajima T, Taniura H, Nishimura I, Yoshikawa K (2004) Necdin interacts with the Msx2 homeodomain protein via MAGE-D1 to promote myogenic differentiation of C2C12 cells. J Biol Chem 279:40484-40493.

Kuwako K, Taniura H, Yoshikawa K (2004) Necdin-related MAGE proteins differentially interact with the E2F1 transcription factor and the p75 neurotrophin receptor. J Biol Chem 279:1703-1712.

Kuwako K, Hosokawa A, Nishimura I, Uetsuki T, Yamada M, Nada S, Okada M,

Yoshikawa K (2005) Disruption of the paternal necdin gene diminishes TrkA signaling for sensory neuron survival. J Neurosci 25:7090-7099.

Lavi-Itzkovitz A, Tcherpakov M, Levy Z, Itzkovitz S, Muscatelli F, Fainzilber M (2012) Functional consequences of necdin nucleocytoplasmic localization. PLoS ONE 7:e33786.

Liu Y, Elf SE, Miyata Y, Sashida G, Liu Y, Huang G, Di Giandomenico S, Lee JM, Deblasio A, Menendez S, Antipin J, Reva B, Koff A, Nimer SD (2009) p53 Regulates Hematopoietic Stem Cell Quiescence. Cell stem cell 4:37-48.

Lopez-Sanchez N, Gonzalez-Fernandez Z, Niinobe M, Yoshikawa K, Frade JM (2007) Single mage gene in the chicken genome encodes CMage, a protein with functional similarities to mammalian type II Mage proteins. Physiol Genomics 30:156-171.

Maruyama K, Usami M, Aizawa T, Yoshikawa K (1991) A novel brain-specific mRNA encoding nuclear protein (necdin) expressed in neurally differentiated embryonal carcinoma cells. Biochem Biophys Res Commun 178:291-296.

Mazumdar J, O'Brien WT, Johnson RS, LaManna JC, Chavez JC, Klein PS, Simon MC (2010) O2 regulates stem cells through Wnt/beta-catenin signalling. Nat Cell Biol 12:1007-1013.

Miyoshi H, Blomer U, Takahashi M, Gage FH, Verma IM (1998) Development of a self-inactivating lentivirus vector. J Virol 72:8150-8157.

Moon HE, Ahn MY, Park JA, Min KJ, Kwon YW, Kim KW (2005) Negative regulation of hypoxia inducible factor-1alpha by necdin. FEBS Lett 579:3797-3801.

Morrison SJ, Csete M, Groves AK, Melega W, Wold B, Anderson DJ (2000) Culture in reduced levels of oxygen promotes clonogenic sympathoadrenal differentiation

by isolated neural crest stem cells. J Neurosci 20:7370-7376.

Mutoh T, Sanosaka T, Ito K, Nakashima K (2012) Oxygen levels epigenetically regulate fate switching of neural precursor cells via hypoxia-inducible factor 1alpha-notch signal interaction in the developing brain. Stem Cells 30:561-569.

Nishimura I, Sakoda JY, Yoshikawa K (2008) Drosophila MAGE controls neural precursor proliferation in postembryonic neurogenesis. Neuroscience 154:572-581.

Nishimura I, Shimizu S, Sakoda JY, Yoshikawa K (2007) Expression of Drosophila MAGE gene encoding a necdin homologous protein in postembryonic neurogenesis. Gene Expr Patterns 7:244-251.

Panchision DM (2009) The role of oxygen in regulating neural stem cells in development and disease. J Cell Physiol 220:562-568.

Pfenninger CV, Roschupkina T, Hertwig F, Kottwitz D, Englund E, Bengzon J, Jacobsen SE, Nuber UA (2007) CD133 is not present on neurogenic astrocytes in the adult subventricular zone, but on embryonic neural stem cells, ependymal cells, and glioblastoma cells. Cancer Res 67:5727-5736.

Reynolds BA, Weiss S (1996) Clonal and population analyses demonstrate that an EGF-responsive mammalian embryonic CNS precursor is a stem cell. Dev Biol 175:1-13.

Reynolds BA, Tetzlaff W, Weiss S (1992) A multipotent EGF-responsive striatal embryonic progenitor cell produces neurons and astrocytes. J Neurosci 12:4565-4574.

Rodrigues CA, Diogo MM, da Silva CL, Cabral JM (2010) Hypoxia enhances proliferation of mouse embryonic stem cell-derived neural stem cells. Biotechnol Bioeng 106:260-270.

Studer L, Csete M, Lee SH, Kabbani N, Walikonis J, Wold B, McKay R (2000) Enhanced proliferation, survival, and dopaminergic differentiation of CNS precursors in lowered oxygen. J Neurosci 20:7377-7383.

Taniura H, Matsumoto K, Yoshikawa K (1999) Physical and functional interactions of neuronal growth suppressor necdin with p53. J Biol Chem 274:16242-16248.

Taniura H, Kobayashi M, Yoshikawa K (2005) Functional domains of necdin for protein-protein interaction, nuclear matrix targeting, and cell growth suppression. J Cell Biochem 94:804-815.

Taniura H, Taniguchi N, Hara M, Yoshikawa K (1998) Necdin, a postmitotic neuron-specific growth suppressor, interacts with viral transforming proteins and cellular transcription factor E2F1. J Biol Chem 273:720-728.

Taylor BL, Zhulin IB (1999) PAS domains: internal sensors of oxygen, redox potential, and light. Microbiol Mol Biol Rev 63:479-506.

Tseng YH, Butte AJ, Kokkotou E, Yechoor VK, Taniguchi CM, Kriauciunas KM, Cypess AM, Niinobe M, Yoshikawa K, Patti ME, Kahn CR (2005) Prediction of preadipocyte differentiation by gene expression reveals role of insulin receptor substrates and necdin. Nat Cell Biol 7:601-611.

Uchida N, Buck DW, He D, Reitsma MJ, Masek M, Phan TV, Tsukamoto AS, Gage FH, Weissman IL (2000) Direct isolation of human central nervous system stem cells. Proc Natl Acad Sci U S A 97:14720-14725.

Uetsuki T, Takagi K, Sugiura H, Yoshikawa K (1996) Structure and expression of the mouse necdin gene. Identification of a postmitotic neuron-restrictive core promoter. J Biol Chem 271:918-924.

Uetsuki T, Takemoto K, Nishimura I, Okamoto M, Niinobe M, Momoi T, Miura M, Yoshikawa K (1999) Activation of neuronal caspase-3 by intracellular

accumulation of wild-type Alzheimer amyloid precursor protein. J Neurosci 19:6955-6964.

Wada T, Haigh JJ, Ema M, Hitoshi S, Chaddah R, Rossant J, Nagy A, van der Kooy D (2006) Vascular endothelial growth factor directly inhibits primitive neural stem cell survival but promotes definitive neural stem cell survival. J Neurosci 26:6803-6812.

Wiesener MS, Jurgensen JS, Rosenberger C, Scholze CK, Horstrup JH, Warnecke C, Mandriota S, Bechmann I, Frei UA, Pugh CW, Ratcliffe PJ, Bachmann S, Maxwell PH, Eckardt KU (2003) Widespread hypoxia-inducible expression of HIF-2alpha in distinct cell populations of different organs. FASEB J 17:271-273.

Zhao T, Zhang CP, Liu ZH, Wu LY, Huang X, Wu HT, Xiong L, Wang X, Wang XM, Zhu LL, Fan M (2008) Hypoxia-driven proliferation of embryonic neural stem/progenitor cells--role of hypoxia-inducible transcription factor-1alpha. FEBS J 275:1824-1834.

Zimmer M, Ebert BL, Neil C, Brenner K, Papaioannou I, Melas A, Tolliday N, Lamb J, Pantopoulos K, Golub T, Iliopoulos O (2008) Small-molecule inhibitors of HIF-2a translation link its 5'UTR iron-responsive element to oxygen sensing. Mol Cell 32:838-848.

Figures

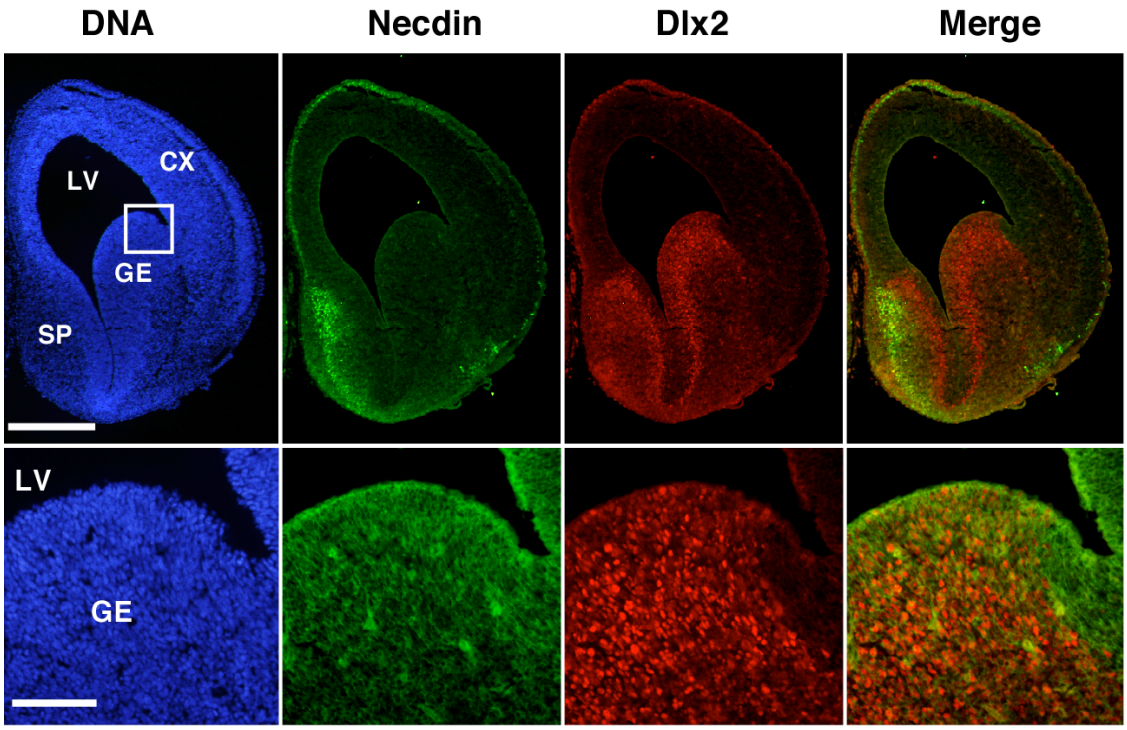

Figure 1. Expression patterns of necdin in embryonic brain.

A, Double immunostaining for necdin and Dlx2. Frozen forebrain sections of E14.5 mouse embryo were double-stained for necdin and Dlx2. Necdin (green) and Dlx2 (red) images were merged (yellow). CX, cortex; LV, lateral ventricle; GE, ganglionic eminence; SP, septum. Scale bars: 500 μm (top), 100 μm (bottom);

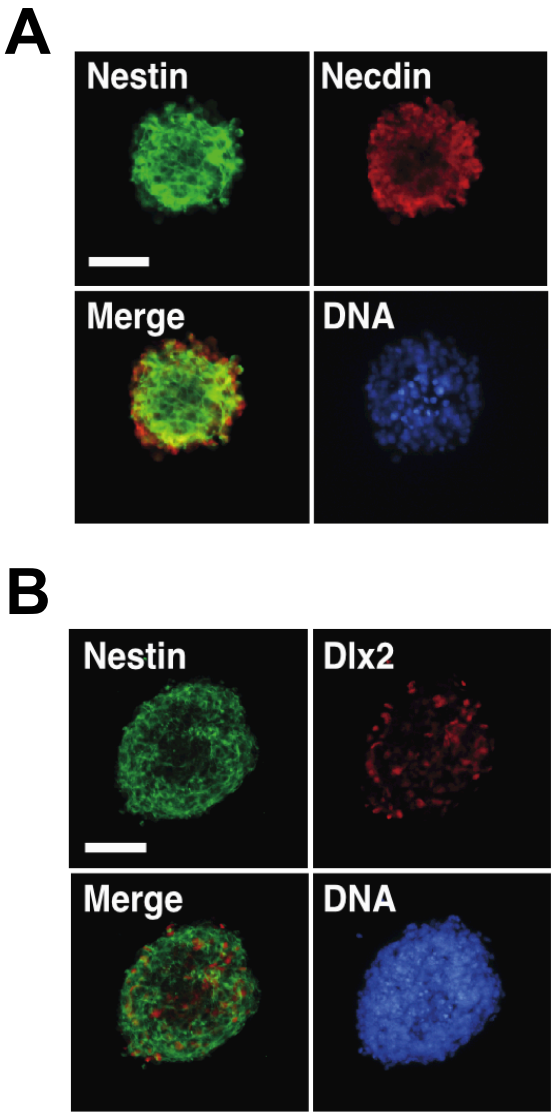

Figure 2. Immunostaining for nestin, necdin, Dlx2 in primary NSCs.

NSCs (6 d culture) in primary neurospheres were immunostained for nestin (green) and necdin (red) (***A***) or Dlx2 (red) (***B***), and two images were merged (yellow). Scale bars: 50 μm

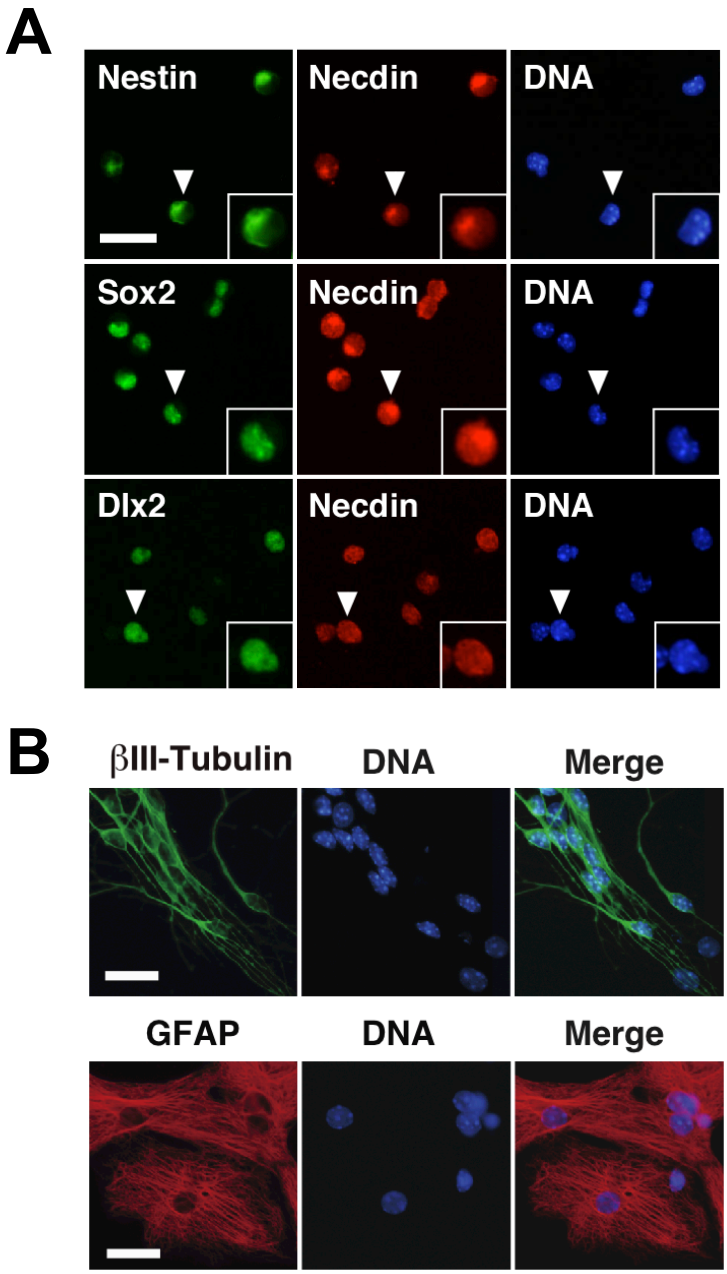

Figure 3. Expression of necdin in primary NSCs.

A, Expression of necdin in NSC markers. Primary neurospheres were dispersed, fixed 2 h later, and double-stained for necdin and nestin, Sox2, or Dlx2. Insets, magnified images of representative cells (arrowheads). Quantitative data are in Results. ***B,*** Immunostaining for βIII-tubulin and GFAP in differentiated cells. Primary cultured NSCs were induced to differentiate in the growth factor-deprived medium for 5 d. The cells were immunostained for βIII-tubulin (green) and GFAP (red). Chromosomal DNA was stained with Hoechst 33342 (DNA). Scale bars: ***A, B,*** 25 μm.

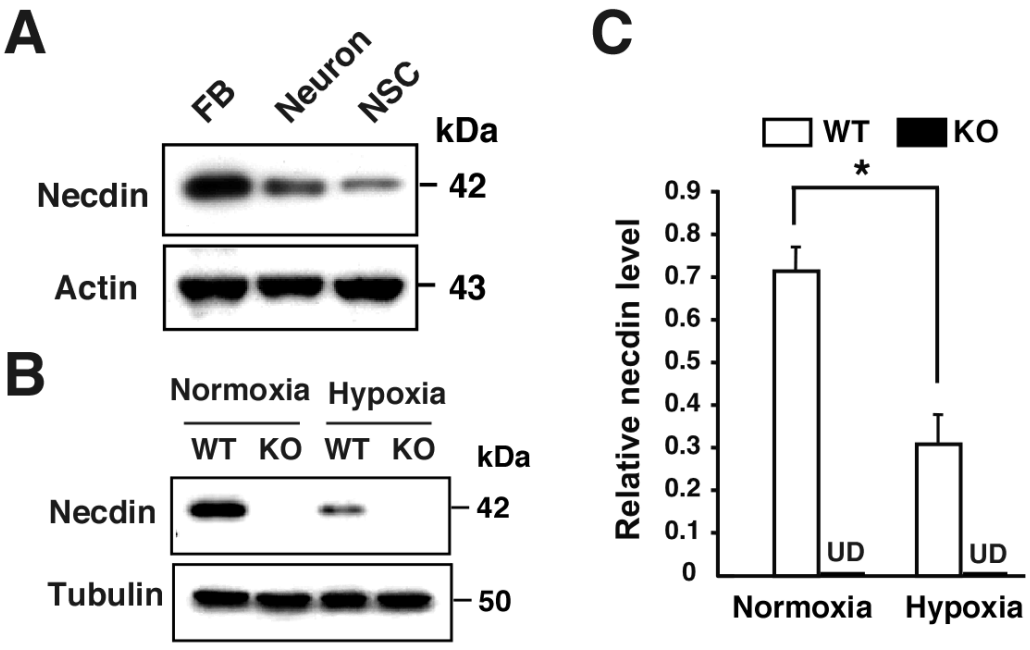

Figure 4. Necdin-deficiency and hypoxia enhance neurosphere formation.

A, Necdin expression in primary NSCs. Expression of necdin and actin in NSCs (NSC) was analyzed by Western blotting using E14.5 mouse forebrain (FB) and primary neurons (Neuron) as positive controls. ***B***, ***C***, Necdin protein levels in normoxic and hypoxic NSCs. Primary NSCs (6 d culture) prepared from wild-type (WT) and *Ndn*-mutant mice (KO) were incubated for 3 d in 20% O_2 (Normoxia) and 2% O_2 (Hypoxia). The cell lysates were analyzed by Western blotting using antibodies to necdin and β-tubulin (***B***). The necdin level was quantified by densitometry and normalized to the β-tubulin level (***C***). UD, undetectable. ***C***, mean ± SEM (n=3). *p < 0.05.

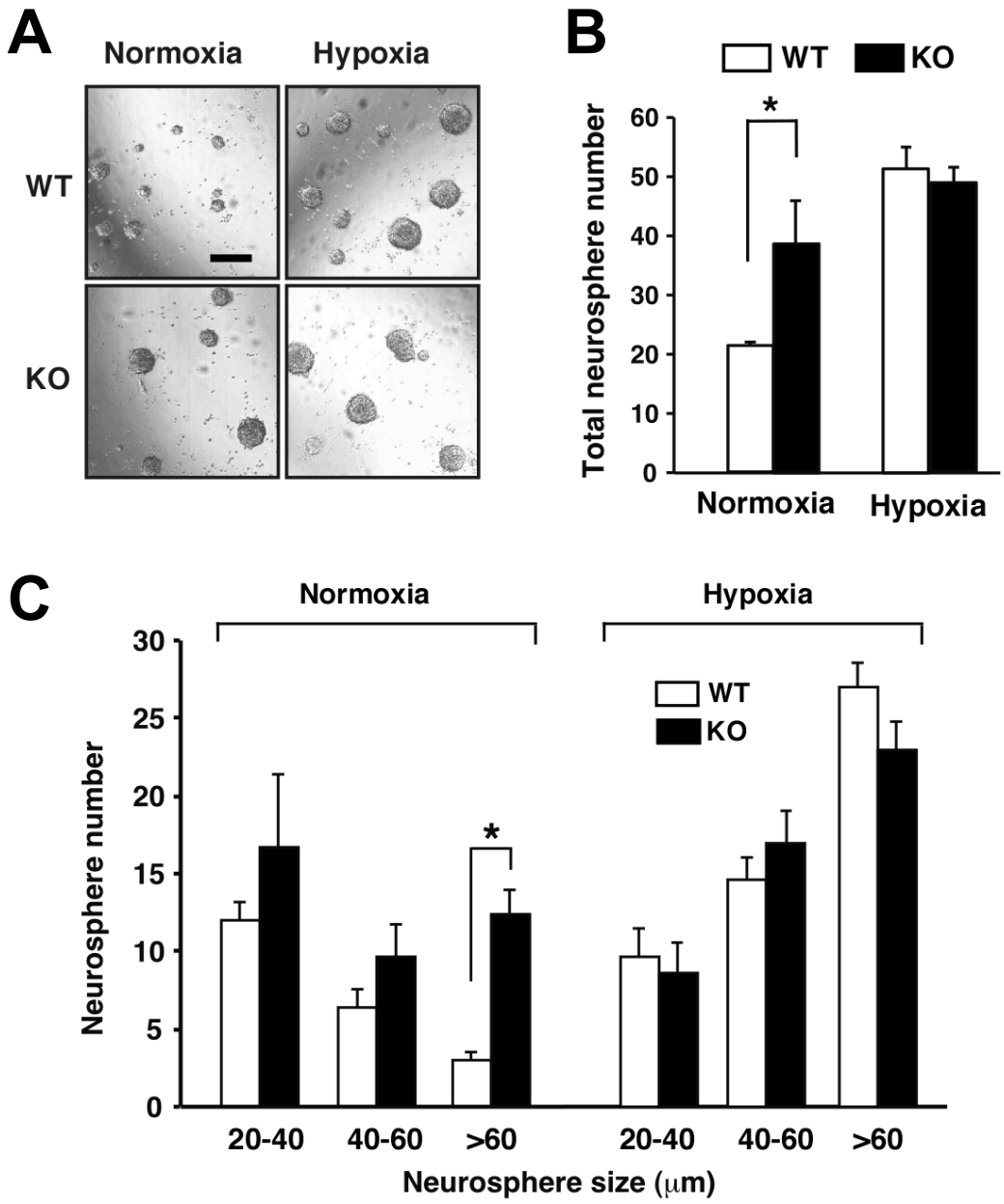

Figure 5. Neurosphere formation assay.

NSCs (6 d culture) were subjected to neurosphere formation assay in normoxia or hypoxia for 5 d. Representative images of NSCs from WT and KO mice are shown (***A***). Scale bar, 200 μm. The total number of neurospheres (>20 μm in diameter) (***B***) and the numbers of three groups (20-40 μm, 40-60 μm, >60 μm in diameter)(***C***) were presented. ***B***, ***C***, mean ± SEM (n=3). *$p < 0.05$.

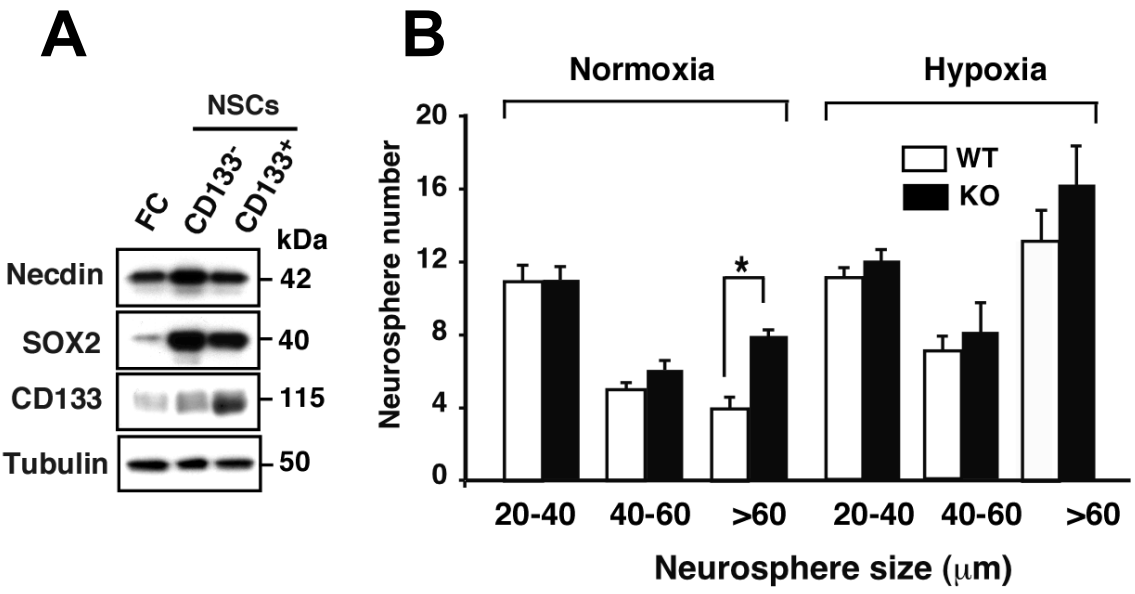

Figure 6. Expression of necdin and Sox2 in CD133$^+$ NSCs and neurosphere assay.

A, Dispersed forebrain cells (FC) were purified using anti-CD133 antibody-coupled microbeads, and unbound (CD133$^-$) and bound (CD133$^+$) cells were cultured for 6 d to obtain NSCs. Protein levels were analyzed by Western blotting. ***B***, Neurosphere assay. CD133$^+$ NSCs were subjected to neurosphere assay in normoxia or hypoxia for 5 d. The numbers of three groups (20-40 μm, 40-60 μm, >60 μm in diameter) were presented. ***B***, mean ± SEM (n=3). *$p < 0.05$.

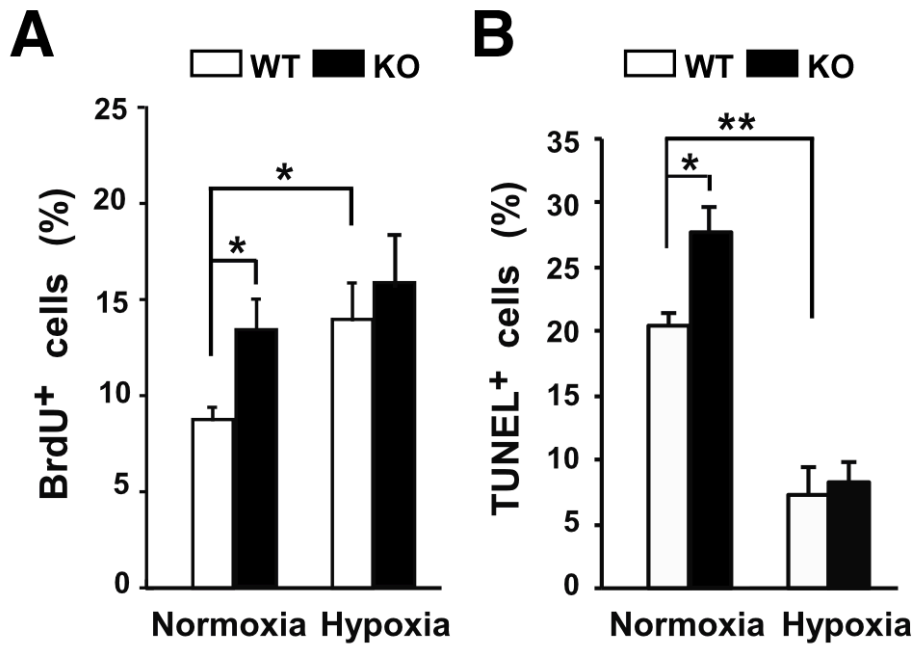

Figure 7. Necdin-deficient NSCs show high rates of proliferation and apoptosis.

A, BrdU incorporation assay. Primary NSCs prepared from WT and KO mice were incubated in normoxia or hypoxia for 24 h, labeled with BrdU for 4 h, and stained for BrdU and chromosomal DNA. BrdU-positive cells (>150 cells analyzed; n=3) were counted. ***B,*** Apoptosis assay. Primary NSCs were incubated in normoxia or hypoxia for 5 d, and subjected to TUNEL assay. TUNEL-positive cells (>300 cells analyzed; n=3) were counted. ***A, B,*** mean ± SEM (n=3). *$p < 0.05$; **$p < 0.01$.

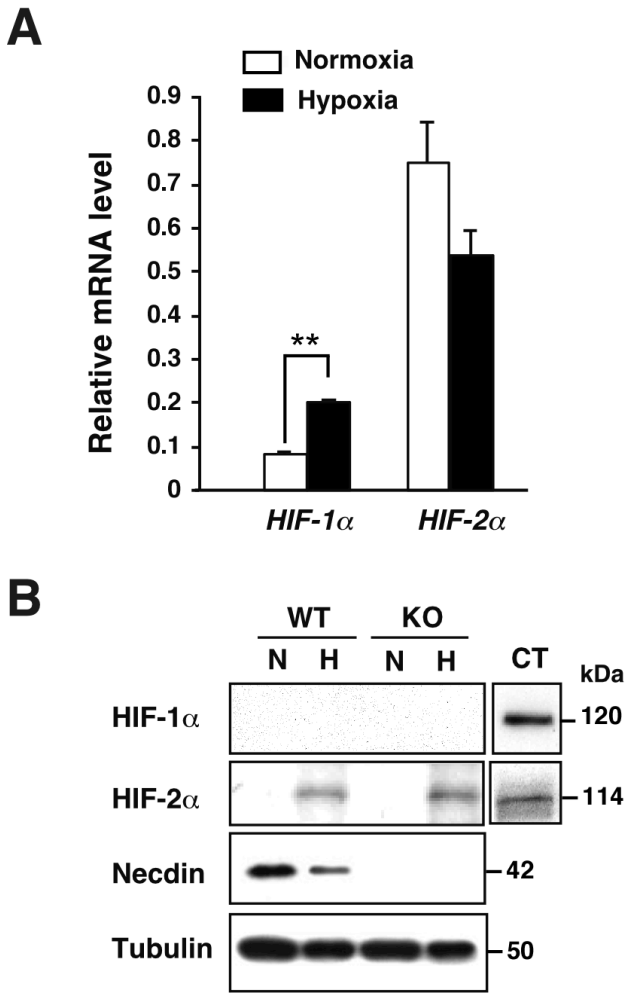

Figure 8. Expression of HIF-1α and HIF-2α in NSCs.

A, *HIF-1α* and *HIF-2α* mRNA levels in NSCs. Primary NSCs (6 d culture) were incubated in 20% O_2 (Normoxia) or 2% O_2 (Hypoxia) for 3 d. *HIF-1α* and *HIF-2α* mRNA levels were analyzed by quantitative RT-PCR. Values were normalized with β-actin mRNA level and corrected with PCR efficiencies. ***B***, Expression of HIF-1α, HIF-2α, and necdin proteins. Primary NSCs (6 d culture) prepared from wild-type (WT) and necdin-null mice (KO) were incubated in normoxia (N) or hypoxia (H) for 3 d. Protein levels were analyzed by Western blotting. CT(control), hypoxic HEK293A cell lysate. ***A***, mean ± SEM (n=3). *$p < 0.05$; **$p < 0.01$.

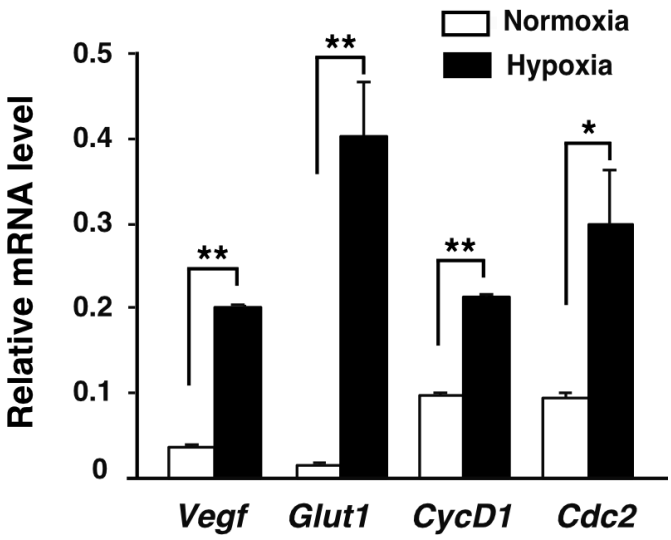

Figure 9. Expression of Vegf, Glut1, Cyclin D1(CycD1), and Cdc2 mRNAs in cultured NSCs.

Primary NSCs (6 d culture) were incubated in normoxia or hypoxia for 3 d. Expression of each mRNA was analyzed by quantitative RT-PCR. Mean ± SEM (n=3). *$p < 0.05$; **$p < 0.01$.

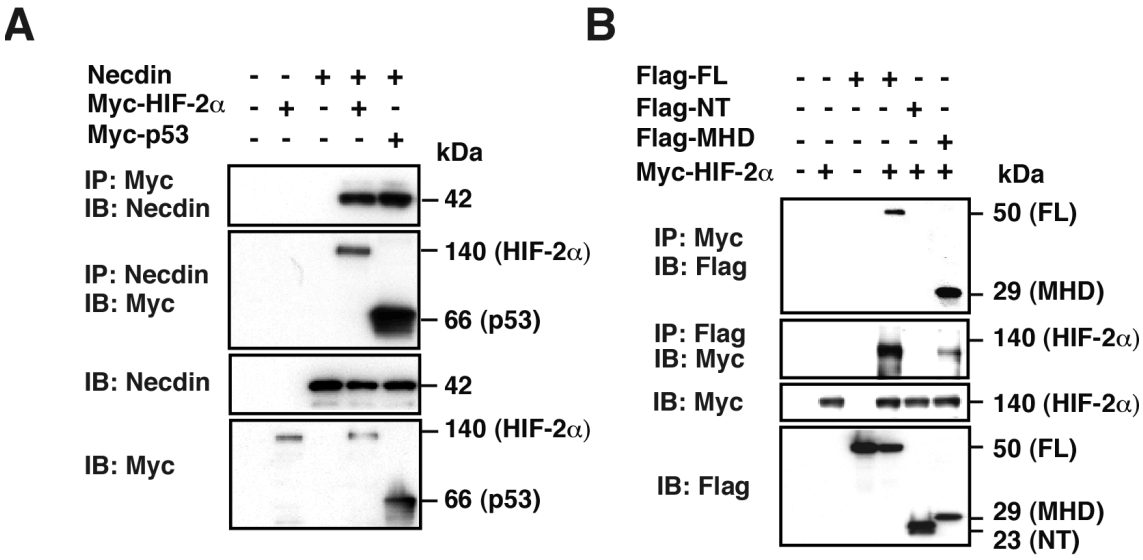

Figure 10. Necdin interacts with HIF-2α via the PAS domain.

A, Interaction between necdin and HIF-2α. HEK293A cells were transfected with expression vectors for necdin, Myc-HIF-2α and Myc-p53 (positive control), and lysates were immunoprecipitated (IP) and immunoblotted (IB) with anti-Myc (Myc) and anti-necdin (Necdin) antibodies. ***B***, HIF-2α-binding domains of necdin. Expression vectors for Flag-tagged necdin full-length 1-325 (FL), N-terminal domain 1-100 (NT) and MAGE homology domain 101-300 (MHD) were cotransfected with HIF-2α cDNA into HEK293A cells, and cell lysates were immunoprecipitated and immunoblotted with anti-Myc (Myc) and anti-Flag (Flag) antibodies.

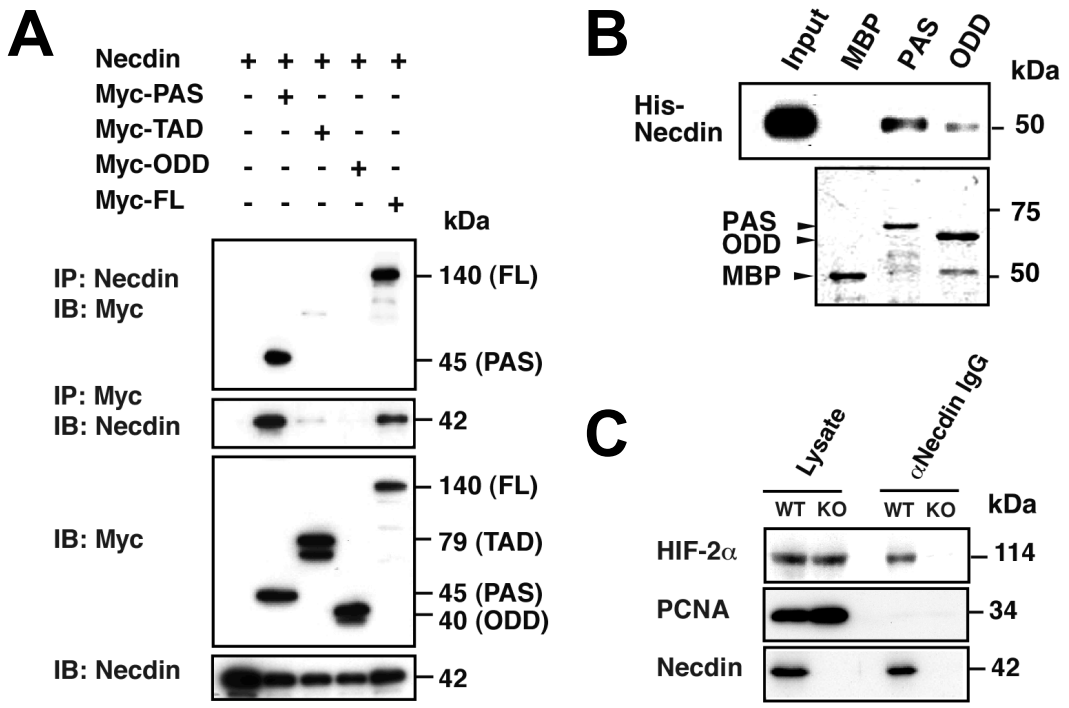

Figure 11. Necdin interacts with HIF-2α via the PAS domain in vivo and in vitro. ***A***, Necdin-binding domains of HIF-2α. Expression vectors for necdin and Myc-tagged HIF-2α PAS domain (PAS), transactivation domain (TAD), oxygen-dependent degradation domain (ODD), or full-length (FL) were transfected into HEK293A cells, and cell lysates were immunoprecipitated and immunoblotted with anti-necdin and anti-Myc antibodies. ***B***, In vitro binding assay. Bacterially synthesized MBP-HIF-2α domains immobilized on amylose resin were incubated with His-tagged necdin. Bound His-necdin was detected with anti-necdin antibody (top). Recombinant proteins were stained with Coomassie Brilliant Blue (bottom). Input, 10% His-necdin. ***C,*** Co-immunoprecipitation assay for endogenous complex containing necdin and HIF-2α. Forebrain nuclear lysates (Lysate) (1 mg) from E14.5 wild-type (WT) and necdin-deficient (KO) mice were immunoprecipitated with GN1 antibody (αNecdin IgG) and detected with antibodies against HIF-2α, PCNA, and necdin.

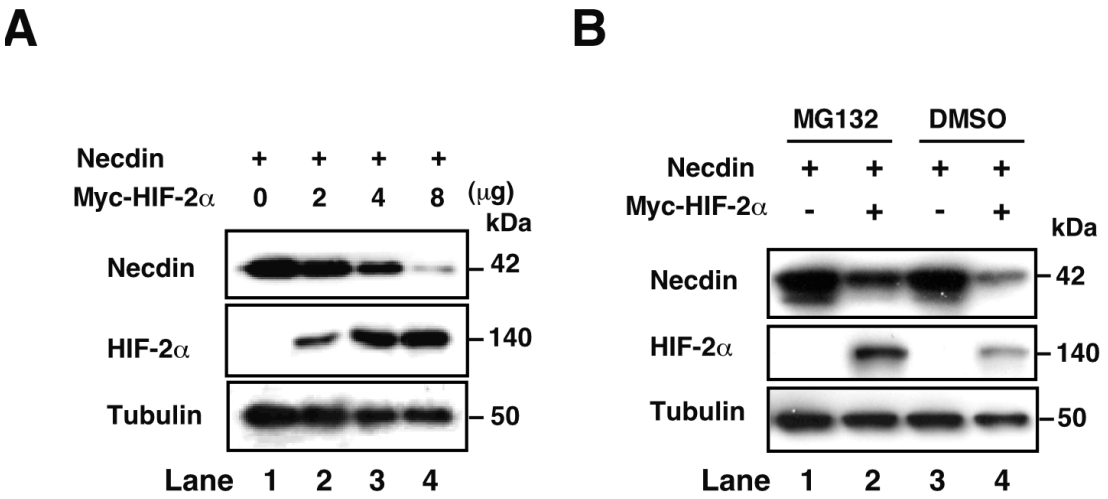

Figure 12. Necdin is degraded via the proteasome pathway.

A, HIF-2α-dependent necdin degradation. Expression vectors for necdin (0.5 μg) and Myc-tagged HIF-2α cDNA (Myc-HIF-2α)(amounts in μg) were transfected into HEK293A cells. Necdin, HIF-2α and β-tubulin levels were analyzed by Western blotting. ***B***, Proteasome-mediated degradation of necdin. HEK293A cells transfected with expression vectors for necdin and Myc-HIF-2α were harvested 24 h later following MG132 treatment for 3 h before harvest. Necdin, Myc and β-tubulin were analyzed by Western blotting. DMSO, vehicle control.

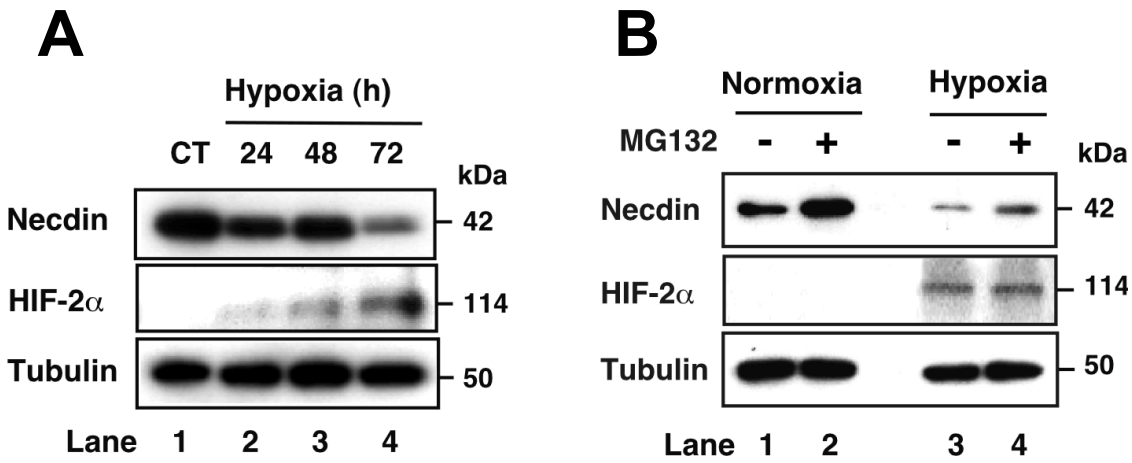

Figure 13. Necdin is degraded via the proteasome pathway in cultured NSCs.
A, Time-dependent necdin degradation. NSCs were prepared and incubated for 24, 48 and 72 h in 2% O_2 (Hypoxia) or for 72 h in 20% O_2 (CT). Necdin, HIF-2α, and β-tubulin levels were analyzed by Western blotting. ***B***, Effects of proteasome inhibition. Primary NSCs (6 d culture) were incubated in normoxia or hypoxia for 72 h, treated with (+) or without (-) MG132 for 24 h before harvest. Necdin, HIF-2α, and β-tubulin levels were analyzed by Western blotting.

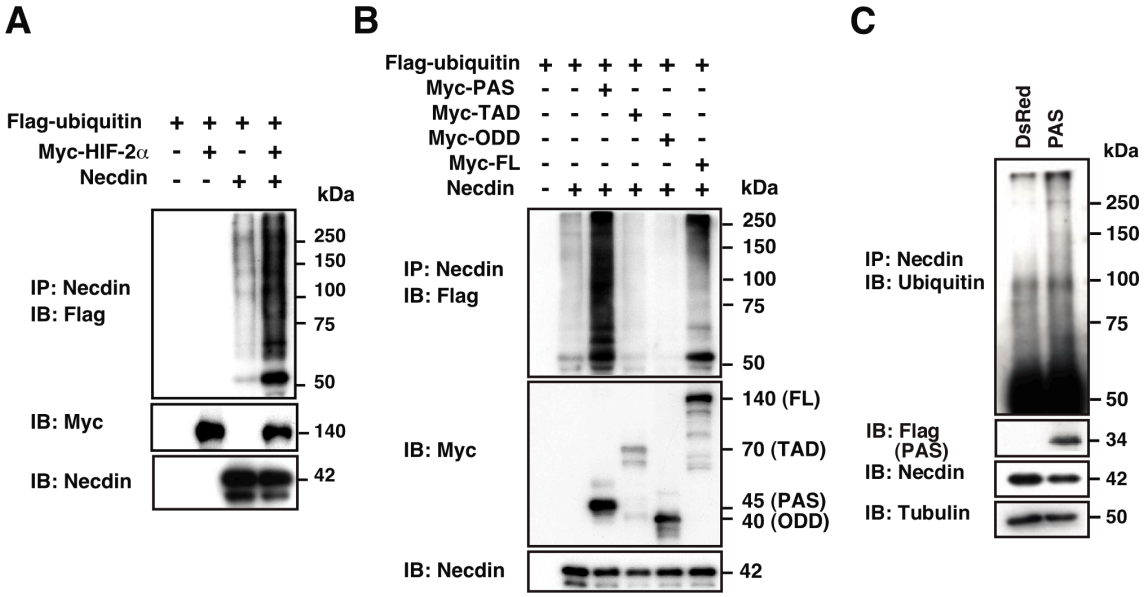

Figure 14. The HIF-2α PAS domain promotes necdin ubiquitination.

A, HIF-2α-enhanced necdin ubiquitination. HEK293A cells transfected with expression vectors for Flag-ubiquitin, Myc-HIF-2α, and necdin were harvested 24 h later following MG132 treatment for 3 h before harvest. Cell lysates were immunoprecipitated with anti-necdin antibody and immunoblotted with anti-Flag antibody. ***B***, PAS domain-mediated necdin ubiquitination. Cells transfected with expression vectors for Flag-ubiquitin, necdin, and Myc-tagged HIF-2α domains (see Fig. ***5C*** for abbreviations) were treated and analyzed as above. ***C***, PAS domain-mediated necdin ubiquitination in NSCs. NSCs were infected with Flag-tagged PAS-expressing lentivirus (PAS) or empty vector (DsRed), and cultured for 6 d in normoxia. Cell lysates were immunoprecipitated with anti-necdin antibody and immunoblotted with anti-ubiquitin antibody.

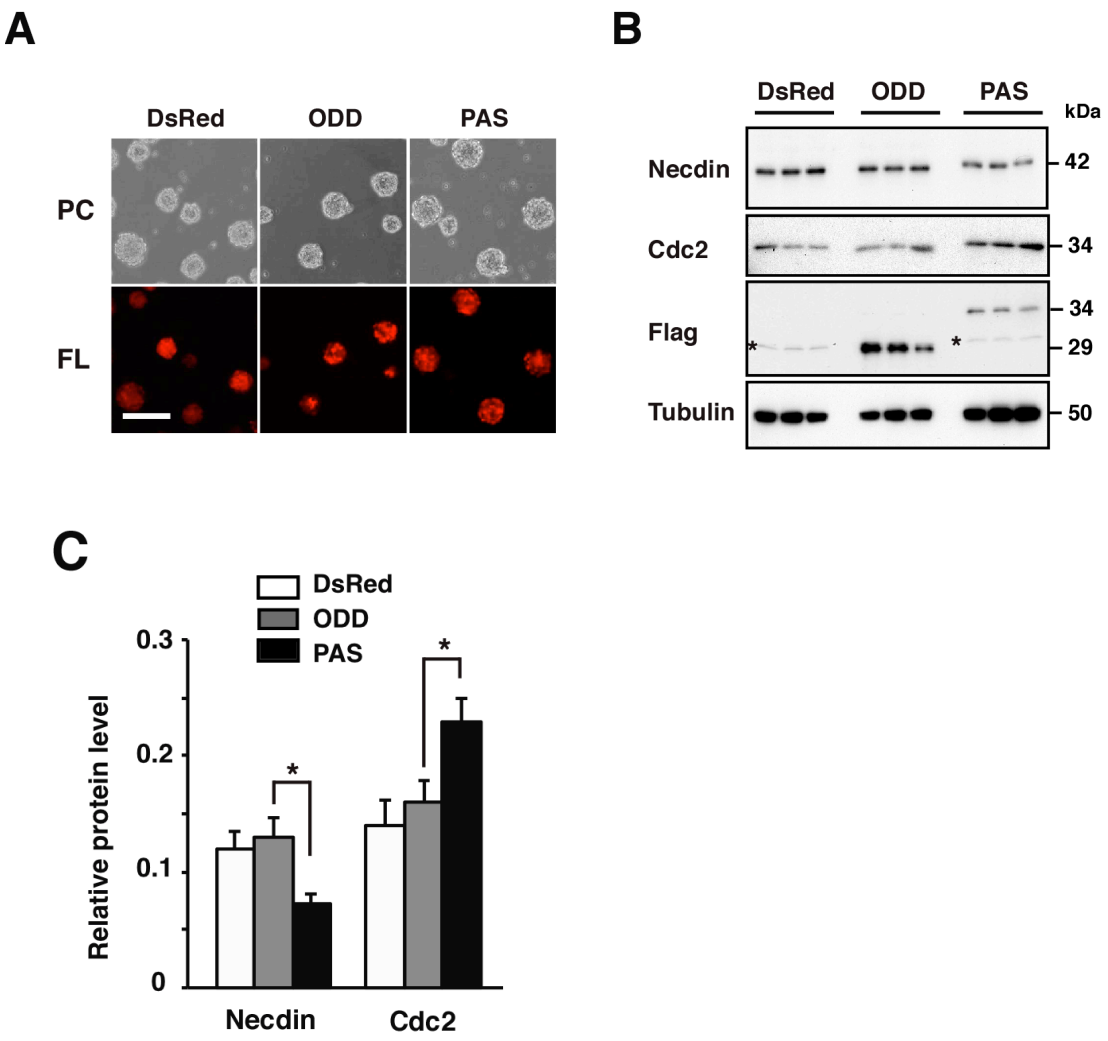

Figure 15. The HIF-2α PAS domain downregulates endogenous necdin level and facilitates NSC proliferation.

A, Lentivirus-infected NSCs. NSCs were infected with lentiviruses expressing DsRed (DsRed, empty vector), Flag-tagged HIF-2α PAS domain (PAS), and Flag-tagged ODD (ODD), and cultured for 6 d. Images of phase-contrast (PC) and fluorescence (FL) of lentivirus-infected NSCs are shown. Scale bar, 100 μm. ***B***, ***C***, Expression of necdin and Cdc2 proteins. Lysates of infected NSCs were analyzed by Western blotting using antibodies to necdin, Cdc2, Flag and β-tubulin (***B***). Asterisks indicate non-specific bands. The protein levels were quantified and normalized to β-tubulin (***C***).

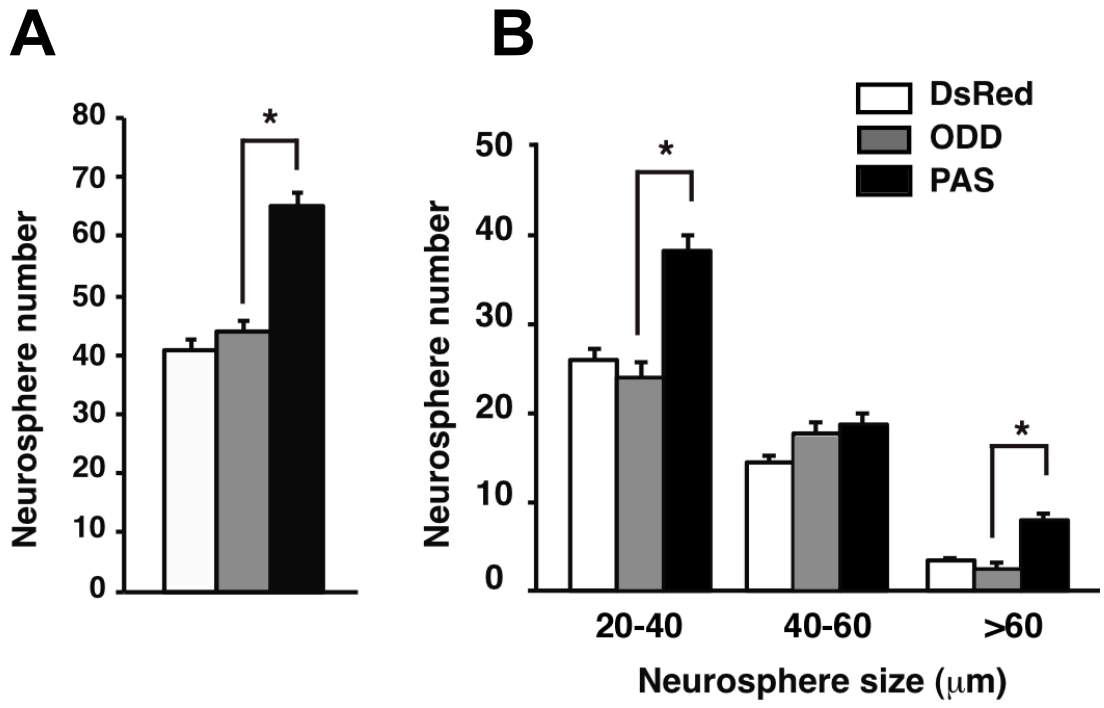

Figure 16. Neurosphere assay.

A, ***B***, Lentivirus-infected $CD133^+$ NSCs were subjected to neurosphere assay in normoxia. The total number of neurospheres (>20 μm in diameter)(***A***) and the numbers of three groups (20-40, 40-60, >60 μm in diameter) were counted (**B**).

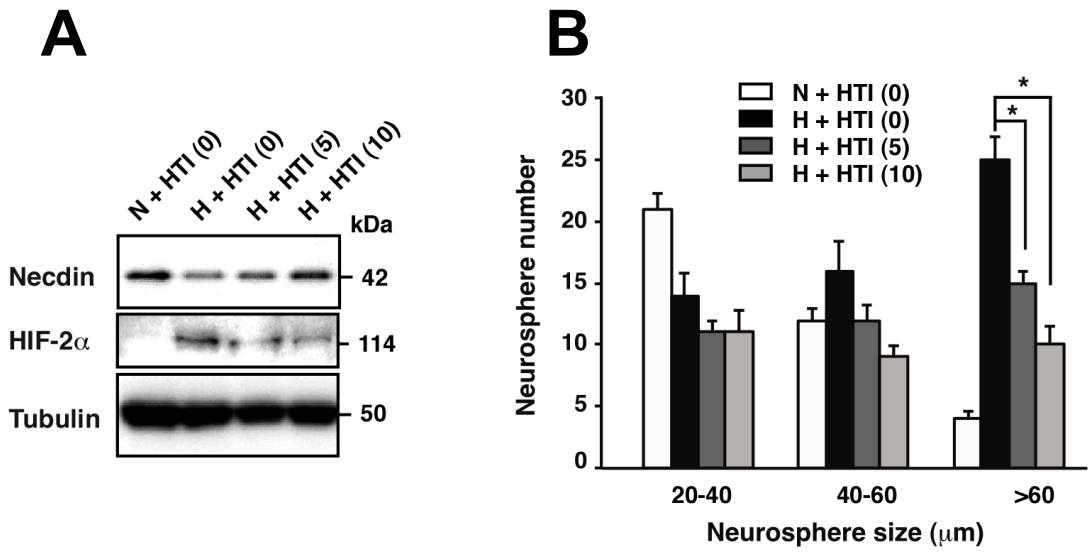

Figure 17. Effects of HIF-2α translation inhibitor.

A, B, Primary NSCs were treated with HIF-2α translation inhibitor (HTI) at 0 (0), 5 (5) and 10 (10) μM for another 3 d in hypoxia (H). Control NSCs were cultured for 9 d in normoxia (N). HIF-2α and necdin were analyzed by Western blotting. ***B***, Neurosphere assay. Primary NSCs were subjected to neurosphere assay in the presence of the translation inhibitor. The numbers of three groups were counted. ***B,*** mean ± SEM (n=3). *$p < 0.05$.

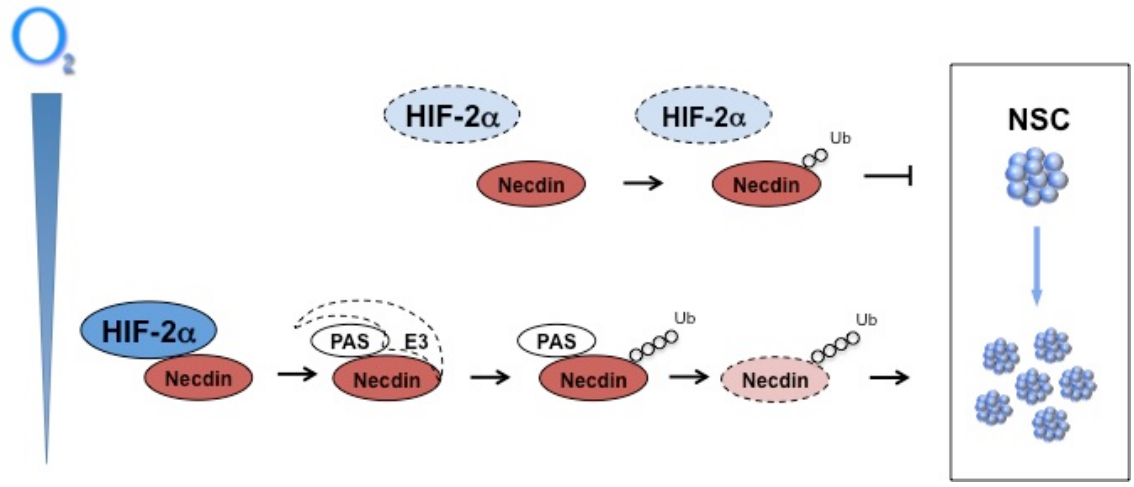

Figure 18. The schematic diagram summarizes the physiological function between HI-2α and necdin

The close interplay between necdin and HIF-2α was demonstrated, which can facilitate the ubiquitination of necdin, and targeting it for proteasomal degradation. The present study suggests that HIF-2α down regulate the expression levels of necdin and cause the degradation, which further affect the proliferation of NSCs cultured under hypoxic conditions.

Acknowledgements

I would like to express my greatest gratitude to the Prof. Kazuaki Yoshikawa who have helped and supported me throughout my project. I am grateful to the Drs. Koichi Hasegawa and Kazushiro Fujiwara for their continuous support, exciting discussion and technical support. I also want to thank Drs. T. Ohkumo and H. Miyoshi for research materials and Ms. K. Imada for technical support.

A special thank to all the members in Prof. Yoshikawa's lab (past or present) who have supported me and brought me a lot of help in Japan.

I wish to thank my parents for their undivided support and interest who inspired me and encouraged me to go my own way, without whom I would be unable to complete my doctoral course.

Finally, I want to thank my friends who motivated me to get success.